

**FIELD INVESTIGATION – EFFECT OF
COEFFICIENT OF CONSOLIDATION AND
RELATIVE DENSITY ON CONE PENETRATION
RESISTANCE**

**A Thesis Submitted to
the Graduate School of
Izmir Institute of Technology
in Partial Fulfillment of the Requirements for the Degree of**

MASTER OF SCIENCE

in Civil Engineering

**by
Hazal TANERİ**

**November 2021
İZMİR**

ACKNOWLEDGMENTS

Firstly, I would like to express my special thanks to my supervisor Assoc. Prof. Dr. Nurhan Ecemiş Zeren, who guided me in scientific terms with her knowledge and experience, as well as supported me with her encouragement and patience throughout this thesis.

I would like to special thanks to the jury members Dr. Volkan İşbuğa and Dr. Devrim Şüfa Erdoğan for their attendance at my thesis seminar and for their valuable recommends for this study.

I would like to special thanks to my father Kamil Taneri, who always encourage me about my decisions and strive to be my side with all his means, and of course my mother Özlem Taneri, who tries to shed light on me during all my life with all her love and ideas, and my brother Altay Taneri who makes me feel hopeful against all difficulties.

My special thanks to Mehmet Önler, who made me believe that there is nothing I cannot achieve when I want to.

Finally, special thanks to Mustafa Karaman and my colleagues Ceren Gizem Sarıtaş, Mustafa Sezer Arık, Ali Hamid Khlaif and Murat Örucü for their supports, knowledge and patience.

ABSTRACT

FIELD INVESTIGATION – EFFECT OF COEFFICIENT OF CONSOLIDATION AND RELATIVE DENSITY ON CONE PENETRATION RESISTANCE

Coefficient of consolidation (c_h) and relative density (D_r) are major parameters to explain soil behavior of silty sands. In this study, it was aimed to compare the effects of c_h and D_r of drained, partially drained and undrained soils on cone penetration resistance and excess pore water pressure. Several field tests; piezocone penetration test (CPTu), standard penetration test (SPT), pore pressure dissipation test (PPDT) and direct push permeability test (DPPT) were conducted on the Northern side of the Izmir Gulf at 20 different locations in 2013 by Ecemis et al. At each location between Cigli and Karsiyaka tests were performed 2.6 m apart from each other.

The cone resistance q_c , the frictional resistance f_s , and pore water pressure behind cone u_2 were obtained from CPTu tests. During the investigation, the effect of c_h obtained from PPDT and DPPT which were conducted at the same depths for each borehole could be examined. SPT tests were used to estimate the D_r of the soil. The disturbed soil samples collected from the boreholes were classified as poorly graded clean sand (SP) to silty sand (SM) and clayey sand (SC).

Results showed that q_c decreased and u_2 increased as the non-dimensional penetration rate ($T = vd/c_h$) increased at the same D_r . From drained to undrained penetration, limit values for the T were determined, and it was seen that T and D_r influenced q_c and u_2 from medium dense to loose silty sands. Also, it was observed that u_2 will be negative for denser silty sands.

ÖZET

ARAZİ İNCELEMESİ – KONSOLİDASYON KATSAYISININ VE GÖRECELİ SIKILIĞIN UÇ PENETRASYON DİRENCİ ÜZERİNE ETKİSİ

Konsolidasyon katsayısı (c_h) ve göreceli sıklık (D_r), siltli kumların zemin davranışını açıklamada ana parametrelerdir. Bu çalışmada, drenajlı, kısmen drenajlı ve drenajsız zeminlerin c_h ve D_r 'nin koni penetrasyon direnci ve aşırı boşluk suyu basıncı üzerindeki etkilerinin karşılaştırılması amaçlanmıştır. Çeşitli saha testleri; piezokon penetrasyon testi (CPTu), direk itme geçirimsizlik testi (DPPT), boşluk basıncı dağılım testi (PPDT) ve standart penetrasyon testi (SPT) 2013 yılında Ecemiş ve diğerleri tarafından İzmir Körfezi'nin kuzey tarafında 20 farklı noktada gerçekleştirilmiştir. Çiğli ve Karşıyaka arasındaki her lokasyonda testler birbirinden 2.6 m aralıklarla yapılmıştır.

Koni uç direnci q_c , sürtünme direnci f_s ve koni arkasındaki boşluk suyu basıncı u_2 CPTu testlerinden elde edildi. Araştırma sırasında, her bir sondaj kuyusu için aynı derinliklerde yürütülen PPDT ve DPPT'den elde edilen c_h 'nin etkisi incelenebilmiştir. Zeminin D_r değerini tahmin etmek için SPT testleri kullanıldı. Sondaj kuyularından alınan örselenmiş zemin örnekleri zayıf gradasyonlu temiz kumdan (SP) siltli kuma (SM) ve killi kuma (SC) kadar sınıflandırılmıştır.

Sonuçlar, aynı D_r değerinde, boyutsuz penetrasyon oranı ($T = vd/c_h$) arttıkça q_c 'nin azaldığını ve u_2 'nin arttığını göstermiştir. Drenajlıdan drenajsız penetrasyona kadar T için sınır değerler belirlenmiş ve T ve D_r 'in, orta yoğunluktan gevşek siltli kumlara kadar q_c ve u_2 'u etkilediği görülmüştür. Ayrıca, daha yoğun siltli kumlar için u_2 'nin negatif olacağı gözlenmiştir.

TABLE OF CONTENTS

LIST OF FIGURES	vii
LIST OF TABLES	ix
CHAPTER 1. INTRODUCTION	1
1.1. Statement of The Problem	1
1.2. Scope of The Study	2
1.3. Thesis Organization	3
CHAPTER 2. BACKGROUND STUDY-EFFECTS OF CONSOLIDATION COEFFICIENT AND RELATIVE DENSITY ON CONE RESISTANCE	4
2.1. Introduction	4
2.2. Change In q_{c1N} and $\Delta u/\sigma_{v0}'$ According to Their Drainage Conditions ...	5
2.3. Change In q_{c1N} and $\Delta u/\sigma_{v0}'$ According to Their Relative Densities	14
2.4. Non-dimensional Penetration Rate	16
2.4.1. Pore Pressure Dissipation Test (PPDT)	17
2.4.2. Direct Push Permeability Test (DPPT)	24
2.5. Relative Density Values Using SPT-(N) ₍₆₀₎	26
CHAPTER 3. INTERPRETATION OF FIELD TEST RESULTS	30
3.1. Introduction	30
3.2. Evaluation of Field Test Results	30
3.2.1. Standard Penetration Test (SPT) Result – D_r	30
3.2.2. Piezocone Penetration Test (CPTu) Result – q_{c1N} and $\Delta u/\sigma_{v0}'$	33
3.2.3. Pore Pressure Dissipation Test (PPDT) Result – c_h	35
3.2.4. Direct Push Permeability Test (DPPT) Result - c_h	41
3.3. Non-Dimensional Penetration Rate	42
CHAPTER 4. EFFECTS OF COEFFICIENT OF CONSOLIDATION and RELATIVE DENSITY ON q_{c1N} and $\Delta u/\sigma_{v0}'$	46
4.1. Introduction	44
4.2. Effect of Consolidation Coefficient On q_{c1N} and $\Delta u/\sigma_{v0}'$	45
4.3. Effect of Relative Density On q_{c1N} and $\Delta u/\sigma_{v0}'$	52
4.4. Conclusion	54

CHAPTER 5. CONCLUSION AND RECOMMENDATION FOR FUTURE	
STUDY	57
5.1. Summary of The Study	55
5.2. Recommendation for Future Study.....	56
REFERENCES	57
APPENDICES	
APPENDIX A. CORRECTED STANDARD PENETRATION NUMBERS AND	
RELATIVE DENSITIES	65
APPENDIX B. UNDRAINED-PARTIALLY DRAINED DISSIPATION CURVES ...	67

LIST OF FIGURES

<u>Figure</u>	<u>Page</u>
Figure 2.1. Normalized cone penetration resistance (q_{c1N}) considering normalized penetration rate ($T=V$)	6
Figure 2.2. The effect of normalized penetration rate on cone resistance	8
Figure 2.3. The variation of excess pore pressure ratio with cone velocity	8
Figure 2.4. Influence of V ($T=V$) on q_{cnet}/σ'_{vy} in soils with different OCR and fines content	9
Figure 2.5. Influence of V ($T=V$) on $\Delta u_2/\sigma'_{v0}$ graph	9
Figure 2.6. The effect of V ($T=V$) on B_qQ ($\Delta u_2/\sigma'_{v0}$)	11
Figure 2.7. Normalized velocity ($T=V$) versus mini-CPT tip resistance (q_c)	12
Figure 2.8. The effect of T on a) $\Delta u/\sigma'_{v0}$ and b) q_{c1N}	13
Figure 2.9. $\Delta u/\sigma'_{v0}$ with $T_0(=T)$ graph	15
Figure 2.10. D_r versus q_c	15
Figure 2.11. The dissipation of pore pressure in OC soils a) Type II b) Type III c) Type IV and Type V	19
Figure 2.12. a) Initial excess pore pressure distribution b) dissipation curves	21
Figure 2.13. The permeameter test equipment with two different diameter probe tips a) $2a= 3.7$ cm b) $2a= 1.2$ cm	23
Figure 3.1. The photo of SPT test truck and SPT tests application in the region between Cigli and Karsiyaka in 2013 taken by Ecemis et al.	28
Figure 3.2. Grain size distribution graph of samples collected from field	29
Figure 3.3. An example curve of how to get t_{50} from dissipation test graphs (SC16, 8.5 m)	33
Figure 3.4. Undrained – partially drained normalized pore pressure dissipation curves that were found from 84 dissipation curves	35
Figure 3.5. a) Type I and b) Type II Undrained – partially drained dissipation curves of silty sands	36
Figure 3.6. Drained excess pore pressure dissipation curves obtained from field	39
Figure 4.1. The graphs of q_{c1N} and $\Delta u/\sigma'_{v0}$ values according to T values a) $10\% < D_r < 25\%$ b) $25\% < D_r < 45\%$ c) $45\% < D_r < 65\%$	45
Figure 4.2. The graph of q_{c1N} according to the method of Sully et al. (1999)	46
Figure 4.3. The graph of q_{c1N} according to the method of Chai et al. (2012a)	46

<u>Figure</u>	<u>Page</u>
Figure 4.4. Trendlines of q_{c1N} and $\Delta u/\sigma_{v0}'$ at average relative densities of 17%, 35% and 55%	47
Figure 4.5. a) q_{c1N} and b) $\Delta u/\sigma_{v0}'$ with T for different average D_r values of 17%, 35% and 55%	50

LIST OF TABLES

<u>Table</u>	<u>Page</u>
Table 2.1. Comparison of drained and undrained T values from literature, methods for obtaining c_h and testing types	14
Table 3.1. Maximum and minimum C_u , D_{50} and FC values and number of samples related to the amount of FC	29
Table 4.1. T values from investigations in literature for undrained and drained penetration	49

CHAPTER 1

INTRODUCTION

1.1. Statement of The Problem

A standard cone penetration test (CPT) is easy to apply for many soil types, from sand to clay in the field. (Lunne et al., 1997) Because the cone penetrometer gives that continuous results through the depth of the measurement. Soil parameters are immediately estimated at the investigation site using CPT, and it provides knowledge about geotechnical design. Measures of the cone penetrometer are defined as the cone tip resistance (q_c), sleeve friction (f_s), and pore pressure (u). The pore pressure measurements can be obtained using the piezocone penetrometer. The piezocone penetration test (CPTu) was proposed by Baligh et al. (1981). And also, it provides to measure at three different locations; the cone tip (u_1), behind the cone (u_2), and behind the friction sleeve (u_3).

The drainage condition affects the cone resistance and excess pore water dissipation during CPT/CPTu in the field. The cone response and pore pressure response vary in silty sand soils called intermediate soils because of the partially drained condition. Although the penetration rate is affected from both the soil's consolidation and permeability, drainage effects have not been clearly understood through the non-dimensional penetration rate yet. Therefore, limits of the non-dimensional penetration rate between the drained and undrained response measured under the same constant speed need to identify. By the way, there are various methods to determine the cone penetration resistance in the laboratory. The non-dimensional penetration rate is applicable to determine the partially drained penetration behavior regardless of the testing methods (Finnie and Randolph, 1994; House et al., 2001; Randolph and Hope, 2004). However, when the different sizes of the cone are used to test, it is not easy to catch the cone's actual response in the laboratory.

The non-dimensional penetration rate is obtained using the coefficient of consolidation (c_h), penetration rate (v), and diameter of the cone (d). In this investigation, penetration speed and diameter size are constant. The partially drained soils can act as

both undrained and drained due to the non-dimensional penetration rate even if v and d parameters are constants. Under undrained conditions, the consolidation coefficient is examined from the results of the pore pressure dissipation test (PPDT). Generally, it is problematic that the consolidation coefficient is obtained from the dissipation test for sandy soil type because sandy soil shows that its excess pore pressure suddenly dissipates during the CPTu. If the consolidation coefficient cannot be directly measured from the dissipation test, the permeability coefficient is used to estimate the consolidation coefficient of sandy soils. A new method called the direct push permeability test (DPPT) to understand the permeability coefficient was proposed by Lee et al. (2008). It provides that the coefficient of permeability of the soil can be directly measured in the field.

The drainage conditions of silty sands and clean sands have to be determined using the relative density of soils. Because the excess pore pressure for undrained penetration shows different behavior under the different relative densities, and this effect causes the different cone penetration responses. Until this study, the effect of relative density on the cone resistance and excess pore pressure of silty sands has not been taken into account so much.

1.2. Scope of The Study

This study mainly focuses on that during CPT, and CPTu cone penetration and excess pore water pressure are affected how much from partially drained conditions and relative density effects. Through the non-dimensional penetration rate, the effects of the coefficient of consolidation and permeability of silty sands and clean sands are considered. The limit values of the non-dimensional penetration from drained to undrained penetration are evaluated considering different relative densities.

1.3. Thesis Organization

The whole thesis includes five chapters. Chapter 1 introduces the thesis that represents the problem that is investigated and the aim of this study.

Chapter 2 shows researches from literature about the cone resistance and excess pore pressure for the non-dimensional penetration rate. Significantly, partially drained

effects are learned how is affected on the dissipation. Simultaneously, dissipation characteristic is deeply searched under the different drainage conditions for silty sand soils.

Chapter 3 mentions that four field tests were conducted at 20 different locations. These are piezocone penetration test (CPTu), pore pressure dissipation test (PPDT), direct push permeability test (DPPT), and standard penetration test (SPT) in silty sands to sandy silts at the northern coast of the İzmir Gulf. The four tests are interpreted to determine the behavior of the cone resistance and excess pore pressure.

Chapter 4 represents that the effects of relative density and coefficient of consolidation are examined on cone response according to results of cone penetration tests. There are some analyses about the cone resistance and excess pore pressure, which are plotted according to their penetration rates by classifying their relative densities.

Finally, the conclusion part of the study summarizes all the results and discussions in Chapter 5.

CHAPTER 2

BACKGROUND STUDY-EFFECTS OF CONSOLIDATION COEFFICIENT AND RELATIVE DENSITY ON CONE RESISTANCE

2.1. Introduction

Piezocene penetration test (CPTu) has been often conducted in the field to determine soil properties. There are many interpretations about the cone penetration resistance for sand or clay soils in Lunne et al. (1997). However, these are not suitable to determine the behavior of silty sand soil because of partially drained conditions. At 2 cm/sec penetration rate, silty soil shows partially drained behavior with regarding to hydraulic conductivity between 10^{-6} and 10^{-3} cm/sec according to Bugno and McNeilan (1984). Therefore, these interpretations cannot be proper to estimate results of geotechnical design in the silty sand field. Drainage conditions are affected from consolidation characteristics or permeability conditions according to fines content. Therefore, the effects of consolidation characteristics have to be clearly examined. At the same time, the relative density is as an important parameter as coefficient of consolidation in sandy soils. It should be well understood to determine the results of the cone penetration test.

In this chapter, the studies that had been carried out so far on cone resistance have been examined. The results of studies investigating the effect of coefficient of consolidation and relative density on cone resistance and excess pore water pressure were compared. A few studies were found to analysis on dissipation of excess pore pressure around the cone that is used to calculate the consolidation coefficient where the silty soil has undrained conditions. It was concluded that different types of dissipation curves can be examined according to the study which is correct for our investigation, and for undrained penetration, the coefficient of consolidation of silty sands can be obtained. As a last one, the methods for the relative density obtained using corrected standard penetration numbers were investigated.

2.2. Change In q_{c1N} and $\Delta u/\sigma_{v0}'$ According to Their Drainage Conditions

In literature, some of investigations were accessible about the relationship between drainage conditions (c_h) and the cone resistance (q_{c1N}) or excess pore pressure ($\Delta u/\sigma_{v0}'$). Some of these researches were experimental, and some were numerical. Also, they were mainly related either sand or clay. Nevertheless, it had been beginning to study in the last 15 years about experimental or numerical investigations for silty sand soils. Experimental investigations belong to Kumar and Bajju (2009); Kokusho et al. (2012); Karaman (2013); Ecemis and Karaman, (2014); Huang (2015) for silty sands and Randolph and Hope (2004); Schneider et al. (2007); Kim et al. (2008); Jaeger et al. (2010); Oliveira et al. (2011) for clay. Numerical investigations belong to Yi et al. (2012); Cecceto and Simonini (2017) for partially drained and Thevanayagam and Ecemis (2008) for silty sands.

Kumar and Bajju (2009) studied that the effect of penetration rate on cone resistance of clean sand or silty sands which had 15% or 25% fines content. They used a miniature cone penetrometer with 19.5 mm in diameter and a large triaxial chamber with 140 mm in diameter. As a result of the study, the cone resistance increased with the increase in penetration rate. Penetration rates which compared their cone resistance were 0.1 mm/s and 0.02 mm/s. However, they did not get the transition from drained to partially drained or to undrained penetration due to that the maximum penetration rate was not enough to trigger. Therefore, the comparison between q_c values for undrained and partially drained or drained penetration was not carried through their study about the effect of penetration rate.

Kokusho et al. (2012) used a miniature cone with diameter of 6 mm in triaxial equipment for performing CPTs and undrained triaxial tests for the same specimen. They aimed to examine the effects of non/low fines content on the cone resistance. According to results of their experiments, the cone resistance decreased and excess pore pressure increased with an increase in fines content of samples for a given relative density. It has to be noticed that even CPT was performed at the highest fines content of 30%, partially drained or even drained penetration was obtained at the diameter of the cone and penetration rate which were small. Again, undrained penetration was not determined even various fines content were used which was known the effect on drainage conditions.

Karaman (2013) and Ecemis and Karaman (2014) proposed a relation the cone resistance (q_{c1N}) with the normalized penetration rate ($T=V$) for silty sands regarding six different relative density ranges. In these studies, c_h values were calculated using permeability coefficient (k) values. If the soil was silty or clayey sand, k value was obtained from PPDT suggested by Parez and Fauriel (1988). Otherwise, DPPT which is a direct measurement method was used to determine k value for clean sand. As a result of the investigation, q_{c1N} decreased significantly when V increased. Because the fines content in soils caused the partially drained penetration and decreased q_{c1N} compared to clean sand. On the other hand, drained to undrained behavior of soils was not clearly obtained for all D_r ranges. For dense to medium dense soils, both V and D_r were a significant influence on q_{c1N} from drained to partially drained penetration. However, it can be said that there was not too much alteration in q_{c1N} above V of 10. Therefore, the transition value from partially drained to undrained was determined as 10 according to the study of Karaman (2013) and Ecemis and Karaman (2014). Nevertheless, for loose soils, only relative density affected on q_{c1N} from partially drained to undrained penetration as it can be seen in Figure 2.1.

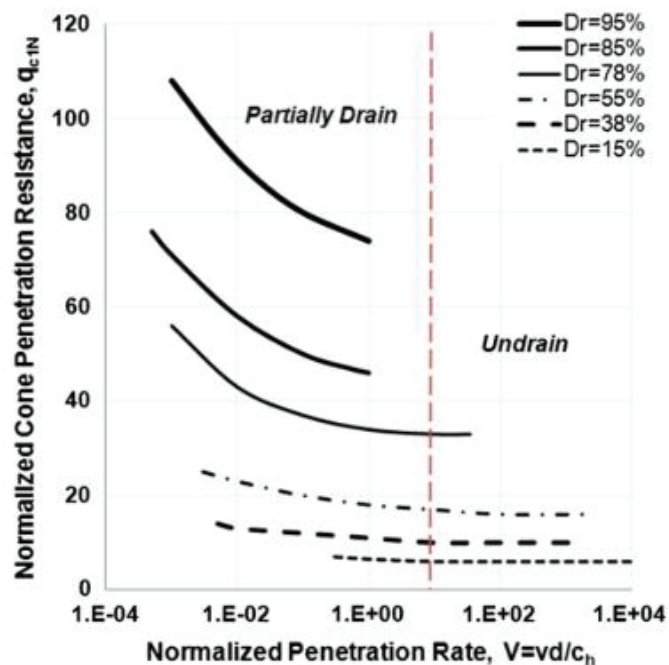


Figure. 2.1. Normalized cone penetration resistance (q_{c1N}) considering normalized penetration rate ($T=V$) (Source: Karaman,2013; Ecemis and Karaman,2014)

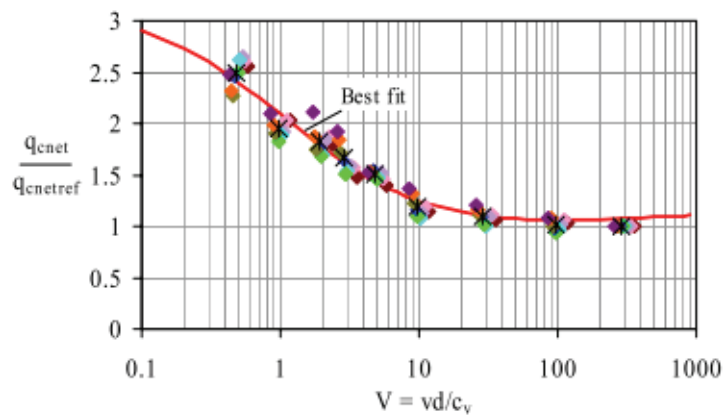
Huang (2015) studied on the liquefaction chart based on CPT calibration chamber tests using a maximum penetration rate of 0.4 cm/sec, and the cone diameter was 1.27 cm. When the experimental model and the numerical model were compared each other, it was observed in the numerical simulation some overestimations of excess pore pressure induced around the cone. Therefore, small cone diameter and small penetration rate can cause just qualitatively evaluation of the effect of fines content on the cone resistance in silty sands. Because different drainage conditions would be occurred. Nevertheless, according to the numerical model, as the normalized penetration rate increased, the cone resistance decreased for a given relative density in partially drainage conditions. Additionally, it was observed that the normalized penetration rate was more appropriate as a main parameter to determine the drainage condition instead of the fines content of silty sands. It was considered to evaluate consolidation characteristics of silty sands for numerical model using the standard penetration rate (2 cm/sec) and the cone diameter size (4.37 cm). For the same relative density, the cone resistance which had smaller c_h values, was smaller than that of bigger c_h ($T = T_0 > 10$). Because of fines content, lower effective stress around cone tip existed due to the fact that the dissipation time of excess pore pressure was longer. In different relative densities, normalized penetration rates could be found for drained and undrained conditions nearly between 0.04 and 10, respectively.

As a result of experimental investigations of silty sands about the effects of drainage conditions on q_{c1N} , it needs an experimental investigation in laboratory which provides field conditions or a field study conducted using the standard penetration rate (2 cm/sec) and the much bigger cone diameter. For this purpose, the results obtained from a series of CPT in the field was used in this study. Before, Karaman (2013) used the same results with different interpretation methods.

Due to the fact that there were not much experimental investigations about the effect of drainage conditions on cone resistance of silty sands, some inferences from experimental studies about that of clay soils were revealed to determine the results of field tests.

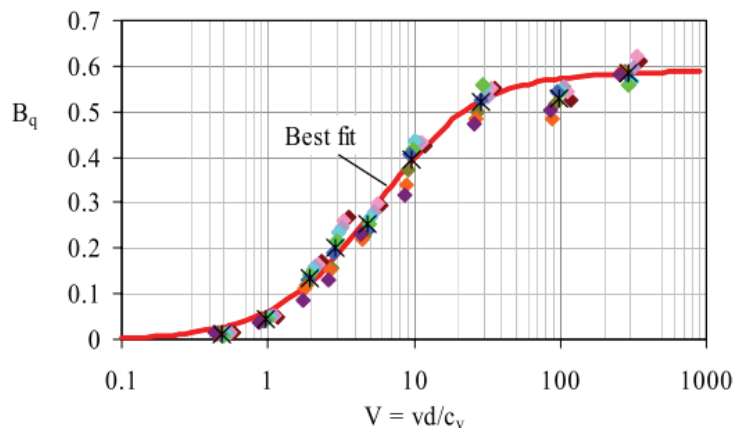
Randolph and Hope (2004) performed a series of model piezocone (cone diameter of 10 mm) and T-bar penetration tests at variable penetration rates in a geotechnical centrifuge to investigate the transition value of normalized penetration rate ($T=V$) of normally consolidated kaolin clay from undrained to partially drained penetration. There was no theoretical basis for the transition curve of cone resistance as a function of V until

this investigation. During the study, c_v values were determined using Rowe cell tests to understand V parameter and compared with the results of a variation of constant rate of penetration test. As a result of constant rate tests, when V decreased, the cone resistance decreased firstly, then it was starting to increase at slower penetration rates because of partial consolidation according to Figure 2.2. Nevertheless, undrained penetration was observed at V of 30 and the excess pore pressure ratio (B_q) of drained penetration was zero at V of 0.3 for cone penetration tests as it can be seen in Figure 2.3.



(a) Cone resistance

Figure. 2.2. The effect of normalized penetration rate on cone resistance
(Source: Randolph and Hope, 2004)



(b) Excess pore pressure ratio, B_q

Figure. 2.3. The variation of excess pore pressure ratio with cone velocity
(Source: Randolph and Hope, 2004)

Schneider et. al. (2007) conducted a series of piezocone penetration tests (cone diameter of 10 mm) in a centrifuge to examine the effect of penetration rate on cone resistance and excess pore pressure of normally consolidated (NC) or over consolidated (OC) kaolin clays and silica flour with bentonite slurry (SFB) at different over consolidation ratio (OCR) and fines contents. Normalized velocity ($T=V$) was calculated according to the coefficient of consolidation (c_v) obtained using permeability of soil (k). They found that the normalized cone tip resistance (q_{cnet}/σ'_{vy}) of all type soils were measured as minimum when V was 100. The vertical yield stress (σ'_{vy}) was used to normalize the net cone resistance (q_{cnet}). When V was bigger than 100, the normalized cone resistance of highly over consolidated soils increased as it can be seen in Figure 2.4. However, undrained normalized excess pore pressure ($\Delta u_2/\sigma'_{v0}$) of NC kaolin clay was just measured at V of 100 as it is shown in Figure 2.5. For drained penetration, $\Delta u_2/\sigma'_{v0}$ of soils was nearly zero at V of 0.1, but fully drained penetration was not achieved until 0.04 in q_{cnet}/σ'_{vy} . Thus, q_{cnet}/σ'_{vy} and $\Delta u_2/\sigma'_{v0}$ were not directly correlated each other for fully drained penetration. In addition, there could be the effect of $\Delta u_2/\sigma'_{v0}$ on q_{cnet}/σ'_{vy} in different OCR and different fines content with an increase in V .

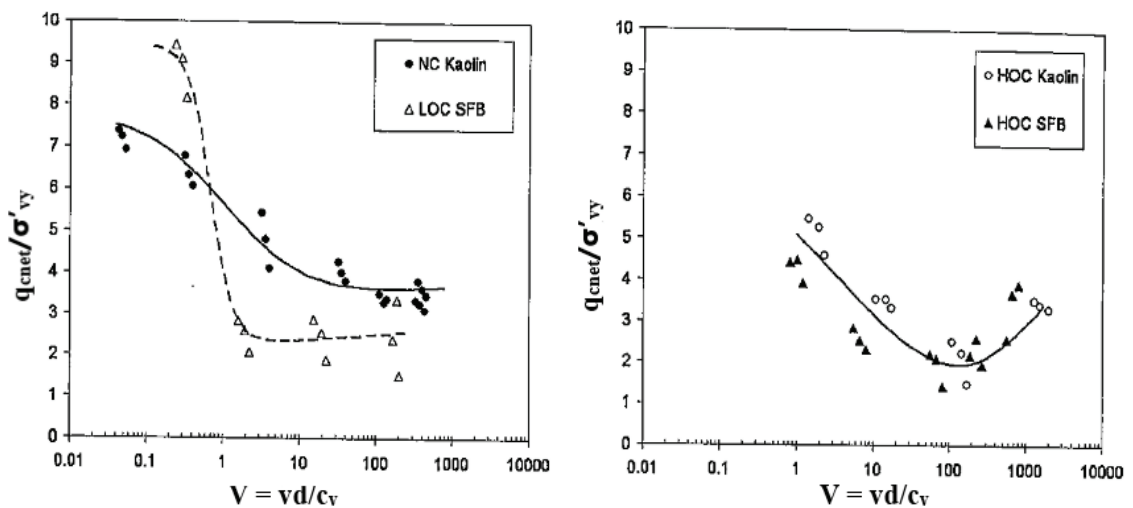


Figure 2.4. Influence of V ($T=V$) on q_{cnet}/σ'_{vy} in soils with different OCR and fines content (Source: Schneider et al., 2007)

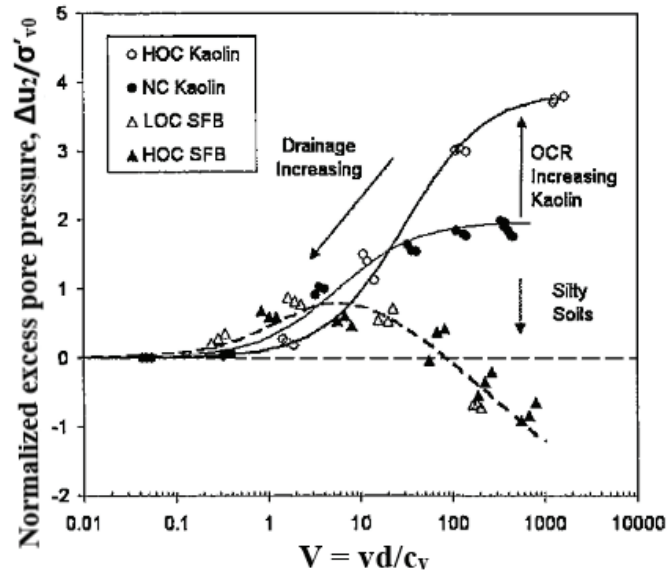


Figure 2.5. Influence of V ($T=V$) on $\Delta u_2/\sigma'_{v0}$ graph

(Source: Schneider et al., 2007)

Kim et al. (2008) conducted a series of CPT with variable penetration rates both in the field and in a calibration chamber to investigate the effects of different penetration rates on cone resistance in clayey soils. To determine normalized penetration rate, oedometer test was used to obtain the coefficient of consolidation (c_v) for two loading layers close to the vertical stress of the corresponding cone penetration test. According to field tests, the normalized cone resistance decreased with increasing normalized penetration rate ($T=V$) until V was nearly equal to 4. Above 4 of V , normalized cone resistance slightly increased with increasing V . However, according to the graph of normalized excess pore pressure, the transition point was at about 10 of V from undrained to partially drained penetration.

In calibration chamber, miniature piezocone with 11.3 mm diameter was conducted for clayey sands with two different mixture ratios. c_v values were obtained from chamber tests. As a result of the chamber tests, from partially drained to drained penetration, the transition point could be defined at 0.05 of V , and 10 of V indicated the transition from undrained to partially drained penetration. At the end of the research, it was deduced that c_v values should be interpreted better for tests performed as partially drained under standard penetration conditions.

Jaeger et al. (2010) performed a centrifuge experiment with 75% sand and 25% kaolin clay using variable penetration rates. During the experiment, c_v values was estimated according to the correlation which used the vertical effective stress and

atmospheric pressure. The normalized cone resistance (Q) decreased with increasing from 0.01 to 160 of normalized velocity ($T=V$). In this study, the viscous effects were absent with increasing to 160 of V against investigations of Randolph and Hope (2004), Schneider et al. (2007) and Kim et al. (2008).

According to Q values, 20 of V indicated the transition point from partially drained to undrained and 0.01 of V indicated from drained to partially drained penetration. In addition, Q_{drained} to $Q_{\text{undrained}}$ ratio was 17, much higher than the previous studies in literature. The relationship between B_q and V was not as clear as the relationship between Q and V . In here, B_q was a pore pressure parameter. However, $B_q Q (\Delta u_2 / \sigma'_{v0})$ parameter showed in Figure 2.6 that the sand-kaolin clay mixture had a negative slope beyond 30 of V was not apparent in B_q - V graph. This was the dilation effect as it was seen before in Schneider et al. (2007).

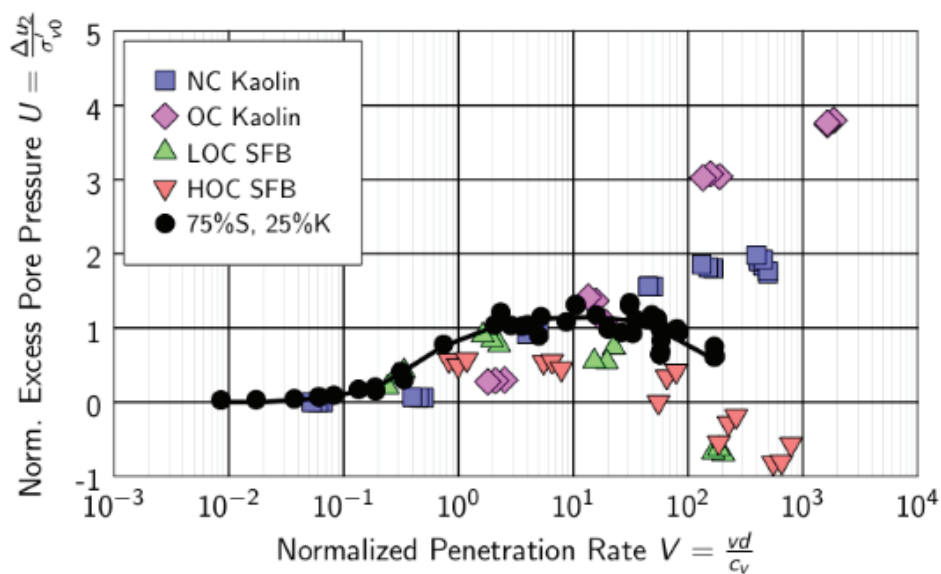


Figure 2.6. The effect of V ($T=V$) on $B_q Q (\Delta u_2 / \sigma'_{v0})$

(Source: Jaeger et al., 2010)

Oliveira et al. (2011) investigated that an analytical approach to the backbone curve equation according test data which had already been fit reported in Oliveira et al. (2006). A series of centrifuge tests with mini-CPT were performed with different penetration rates. Soil was classified as silty clay, clay or clayey silt presented in here according to piezocone tests. As a result of their study about the cone penetration with variable penetration rates of soils, they showed that the tip resistance decreased in the range 1.0 to 75 of normalized penetration rate ($T=V$) because of partially drained

conditions. However, for undrained penetration, the tip resistance of silty clays showed a stabilization trend with a slightly increase when normalized penetration rate was higher than 75 in Figure 2.7 as Randolph and Hope (2004), Schneider et al. (2007) and Kim et al. (2008). It indicated the characteristic viscous effect of the undrained penetration. Still, this topic is needed more investigation to determine an appropriate value for the coefficient of consolidation during the penetration with variable rate.

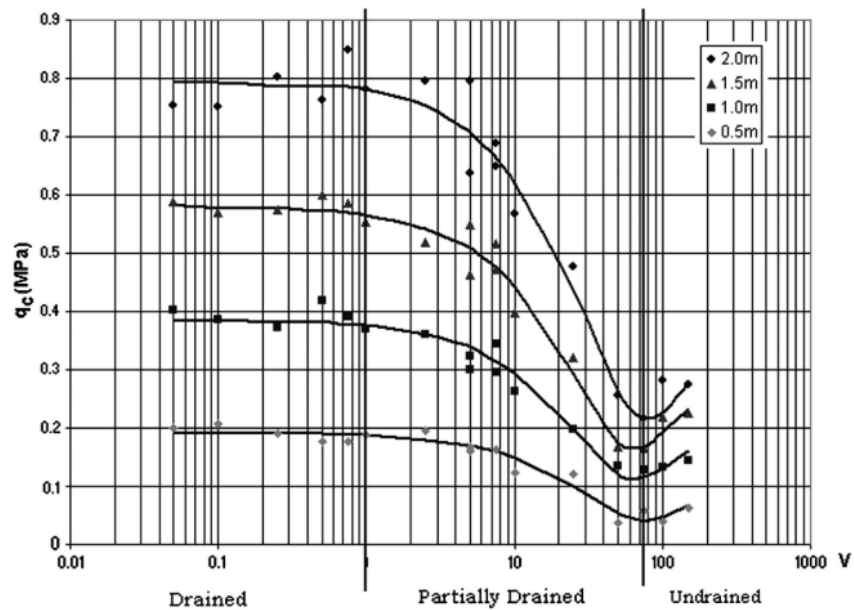


Figure 2.7. Normalized velocity ($T=V$) versus mini-CPT tip resistance (q_c)
(Source: Oliveira et al., 2011)

Numerical investigations which have been interested in partially drained behavior of soils were evaluated to compare results obtained from experimental investigations. For example; even if two soils have the same liquefaction potential or the same stress-strain relation, they may have different the degree of drainages because of differences in coefficient of consolidation. Therefore, different cone resistances (q_{c1N}) are obtained. Thevanayagam and Ecemis (2008) studied that the effects of permeability (k) and consolidation coefficient (c_h) on q_{c1N} at the similar liquefaction potential with consideration of the dilation angle. Numerical simulations were conducted at a constant penetration speed of 2 cm/sec according to standard of the cone penetration with 4.37 cm diameter of the cone. As a result of the study, for dense soil, q_{c1N} decreased with an increase in normalized penetration rate (T) much more than that was for loose soil. At the same density, q_{c1N} for low permeable silty sand was smaller than that was highly

permeable for clean sand. This was the effect of fines content on q_{c1N} as it can be seen in Figure 2.8(b). Because low c_h values caused lower effective stress around the cone in silty sands than clean sands. Excess pore pressure ($\Delta u/\sigma'_{v0}$) had the feature of partially drained penetration when the penetration rate value was between 0.01 and 5. For loose soils, beyond the value of penetration rate was in the range of 5 to 10, $\Delta u/\sigma'_{v0}$ was little affected from increment in T and nearly undrained response could be observed. On the other hand, for dense soils at the same value of T , excess pore pressure was negative and unaffected by the further increase in T . This indicated that the soil had highly dilative response.

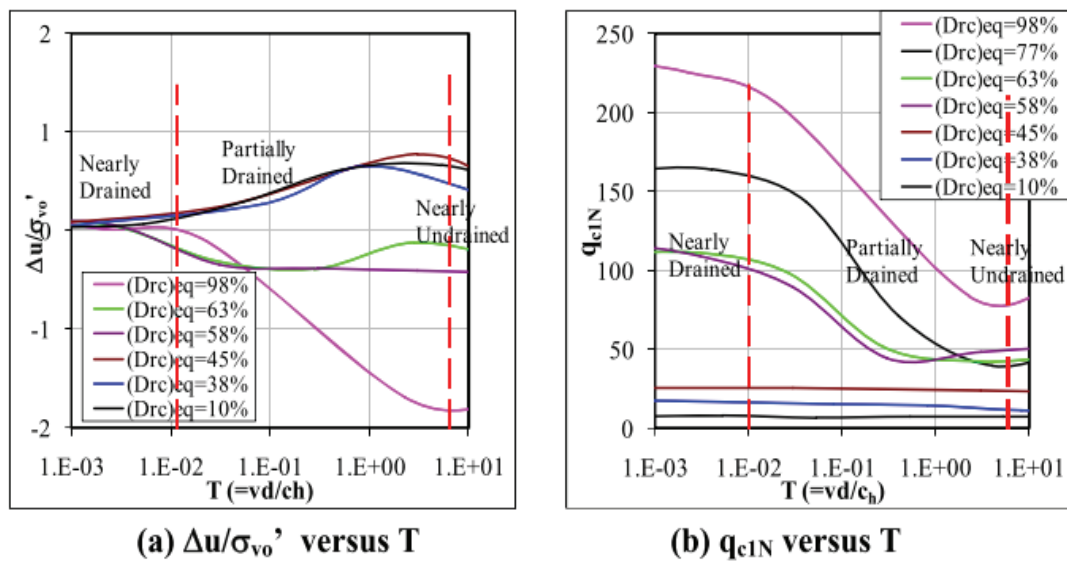


Figure 2.8. The effect of T on a) $\Delta u/\sigma'_{v0}$ and b) q_{c1N}

(Source: Thevanayagam and Ecmis, 2008)

Yi et al. (2012) studied the effects of excess pore pressure (Δu) induced around the cone and dissipation on the cone resistance (q_c) because of variable penetration rates. In order to develop the theoretical transition curve, the numerical model results were used with non-dilative parameters. The maximum penetration speed was 1 mm/sec which was much slower than that applied in situ measurements. However, the cone diameter used herein was larger than that used field measurements. Therefore, non-dimensional velocity ($T=V$) was used to account the different cone size. The coefficient of consolidation (c_v) was deduced according to the equation based on the coefficient of permeability to evaluate partially drained response. In this study, the results were consistent with previous studies in literature that q_c increased with decreasing in V and Δu . Additionally, undrained penetration was observed for normalized cone resistance (q_{cnet}/q_{ref}) at 10 of V . But this

study could not be applicable for highly dilative soils because dilation angle was not taken into account during the numerical analysis.

Cecceto and Simonini (2017) had conducted the numerical model to examine the partially drainage effects on cone penetration resistance and excess pore pressure. Drainage conditions of soils were investigated using permeability coefficient (k) during the penetration rate was keeping the standard velocity of 2 cm/sec. They found transition points of the cone resistance ratio (q_{cnet}/q_{ref}) and the excess pore pressure ratio ($\Delta u_2/\Delta u_{ref}$) as 0.2 and 60 of normalized penetration velocity ($T=V$) for drained and undrained limits, respectively.

According to investigations which were related to partially drained behavior, silty sands need more studies. Because numerical investigations showed that from partially to undrained penetration of clay soils were different from partially penetration of silty soils, and experimental studies of silty sands supported this inference. However, the cone penetration of silty sands has to be examined at standard penetration rate (2 cm/sec) as an experimental study. Table 2.1 was added to compare all investigations were made until present.

Table 2.1. Comparison of drained and undrained T values from literature, methods for obtaining c_h and testing types

Reference	Soil Type	Test Type	c_h obtained from	T for undrained	T for drained
Randolph and Hope, 2004	NC Clay	Centrifuge	Rowe cell test	>30	<0.3
Schneider et al., 2007	NC and OC Clay	Centrifuge	Using k values	>100	-
Ecemis, 2008	Silty sand	Numerical	Using k values	>5	<0.01
Kim et al., 2008	Clay	Calibration Chamber	Chamber test	>10	<0.05
Kumar and Bajju, 2009	Silty sand	Triaxial Chamber with Minicone	-	-	-
Jaeger et al., 2010	Clay	Centrifuge	Empirical Correlation	>20	<0.01
Oliveira et al., 2011	Clay	Centrifuge		>75	<1
Yi et al., 2012	-	Numerical		>10	<0.1
Kokusho et al., 2012	Silty sand	Minicone Cyclic Triaxial	-	-	-
Karaman, 2013	Silty sand	In-situ	Using k values	>10	-
Ecemis and Karaman, 2014	Silty sand	In-situ	Using k values	>10	-
Huang, 2015	Silty sand	Calibration Chamber	Using k values	>10	<0.04
Cecceto and Simonini, 2017	-	Numerical	Using k values	>60	<0.2

2.3. Change In q_{c1N} and $\Delta u/\sigma_{v0}'$ According to Their Relative Densities

In literature, it could be clearly seen that the relative density affected existence of $\Delta u/\sigma_{v0}'$ during cone penetration. Then, q_{c1N} indicated different results under different conditions of relative density.

For medium dense to dense soil, negative excess pore pressure was observed in Figure 2.8(a) Thevanayagam and Ecmis (2008). Even if for loose to dense soil, $\Delta u/\sigma_{v0}'$ was zero in drained penetration, it was changed with respect to its relative density during partially drained penetration. According to this result, it could be said that $\Delta u/\sigma_{v0}'$ of silty sands existed dilative behavior regarding to their relative densities from partially drained to undrained penetration. At the same time, the amount of change in q_{c1N} depended on relative density of silty sand. In general manner, as the relative density was bigger than 50 – 60 %, negative excess pore pressure occurred around the cone and this caused the bigger cone resistance because of the highest effective stress.

Huang (2015) also proposed that for medium dense to dense soils, negative $\Delta u/\sigma_{v0}'$ was observed as seen in Figure 2.9 from drained to undrained penetration which was indicated between 0.04 and 10 because of dilative behavior. In addition, it could be said that for the same T_c , q_{c1N} and $\Delta u/\sigma_{v0}'$ of soils were changed regarding to their relative densities because their fines contents were same. When negative $\Delta u/\sigma_{v0}'$ occurred, q_{c1N} was bigger because of high amount of effective stress around the cone as said by Thevanayagam and Ecmis (2008).

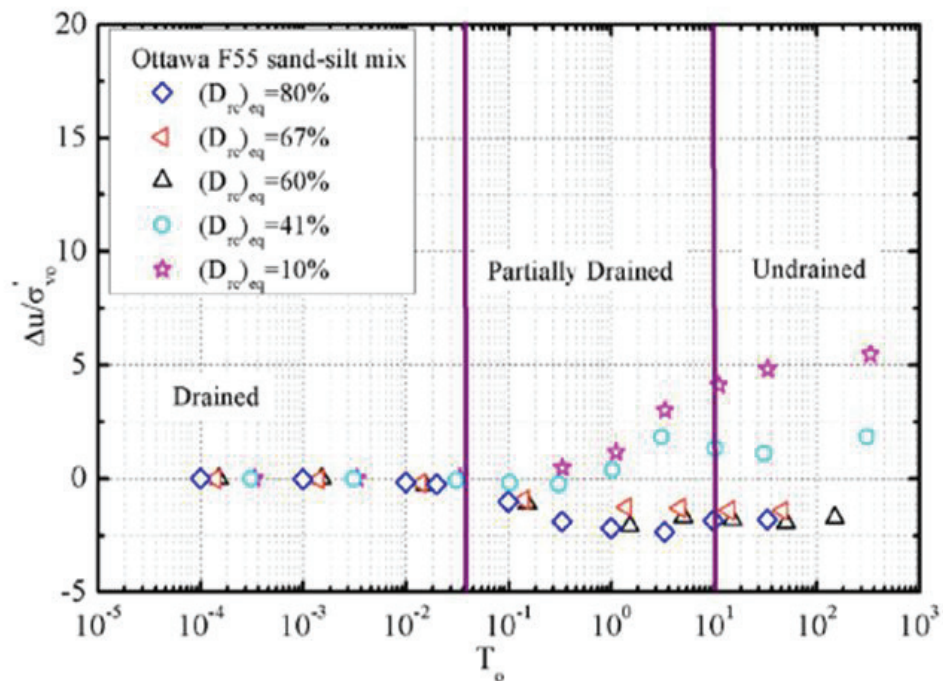


Figure 2.9. $\Delta u/\sigma_{v0}'$ with $T_c (=T)$ Graph

(Source: Huang, 2015)

Karaman (2013) and Ecemis and Karaman (2014) also studied the effect of D_r on q_{c1N} . They proposed that the amount of q_{c1N} of silty sands and clean sands were not change significantly below D_r of 40% according to Figure 2.1.

In the study of Kokusho et al. (2012), it was noted that when the relative density increased, the cone resistance increased regardless the fines content as it can be seen in Figure 2.10.

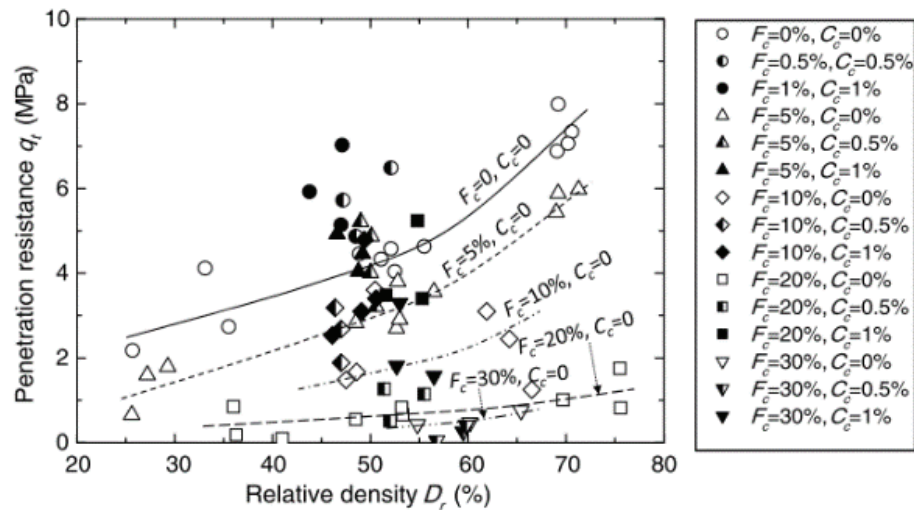


Figure 2.10. D_r versus q_c
(Source: Kokusho et al., 2012)

Krage and Dejong (2016) nearly obtained same results about the relation between excess pore pressure and normalized penetration rate with some differences as Thevanayagam and Ecemis (2008) and Huang (2015). The effect of the relative density of silty sands were not used on this relation even if Krage and Dejong (2016) observed the negative excess pore pressure in dilative soils. The relative density was directly related to the normalized penetration rate. It was observed that the relative density in drained penetration was bigger than that was the partially drained penetration.

2.4. Non-dimensional Penetration Rate

Throughout the investigation, the non-dimensional penetration rate (T) was used to determine the effect of c_h on q_{c1N} and $\Delta u/\sigma_{v0}$. T parameter defined below as include

such non-soil-property properties as penetration rate of the cone (v) and the cone diameter (d);

$$T = \frac{vd}{c_h} \quad (2.1)$$

T parameter which is major to examine drainage conditions of soils was proposed by Finnie and Randolph (1994), House et al. (2001) and Randolph and Hope (2004). In this formula, the coefficient of consolidation (c_h) is the key parameter if non-soil-properties do not affect the drainage condition due to being constant. Thus, soil properties were tried to be observed with respect to the c_h parameter which is hard to obtain. In this study, c_h values were obtained from PPDT from partially drained to undrained penetration and DPPT from drained to partially drained penetration. These test methods have to be correctly understood to determine c_h values.

2.4.1. Pore Pressure Dissipation Test (PPDT)

Pore pressure dissipation test (PPDT) was used to determine c_h values according to the behavior of excess pore pressure (Δu) deduced the cone penetration. Three locations on the cone could be used to measure pore pressure dissipation during the stopped penetration: 1) the cone tip (u_1) 2) behind the cone tip (u_2) and 3) behind the friction sleeve (u_3). In literature, there were some investigations about the position of the behind of the cone (u_2) was more consistent to measure pore pressure dissipation. Baligh et al. (1981) said that the pore pressure measured at the cone tip (u_1) did not affect the cone resistance. They used the measured pore pressure (u_1) to define the identification of soil stratigraphy. The study of Randolph and Hope (2004) showed the similar result with Baligh et al. (1981). Deducing of the c_h was discussed as a consequence of their study was that u_1 position of the cone was better for identifying the soil type, and u_2 position was a prior to deducing values of consolidation coefficient.

PPDT gives us the relationship between Δu and the time of pore pressure dissipation. This relationship can be useful to induce the horizontal coefficient of permeability (k_h) using the formula proposed by Parez and Fauriel (1988);

$$k_h = \frac{1}{(251t_{50})^{1.25}} \quad (2.2)$$

where;

t_{50} = the half time of pore pressure dissipation

Karaman (2013) and Ecemis and Karaman (2014) preferred c_h values obtained using the k values according to this formula. Nevertheless, the half time of pore pressure dissipation (t_{50}) can be interpreted to directly determine c_h values of soils. The dissipation curve is plotted using normalized excess pore pressure values got with respect to the difference of the initial excess pore pressure according to Lunne et al. (1997). In general, the curve is observed monotonically decreasing pore pressure during the dissipation in soft, fine-grained silts and clays. However, in heavily over consolidated silts and clays, the dissipation curve firstly increases and after decreases in time. These curves were named as non-standard dissipation curves in literature. There were some investigations to explain the reasons of this behavior of pore pressure and examine correct t_{50} values into apply the method of Teh and Houlsby (1991) if the non-standard dissipation occurred;

$$c_h = \frac{T_{50} r^2 \sqrt{I_r}}{t_{50}} \quad (2.3)$$

where;

T_{50} = time factor for the half time of pore pressure dissipation

r = radius of the cone

I_r = rigidity index

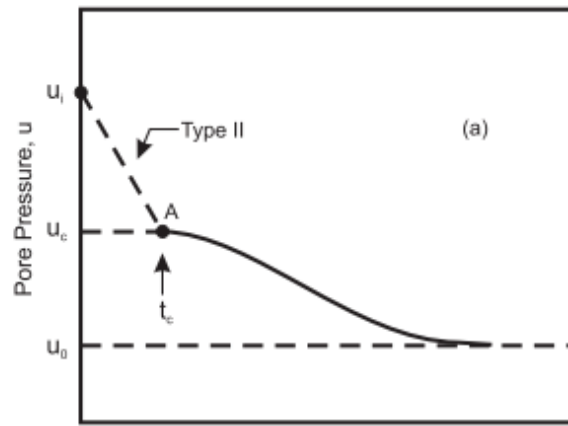
Burns and Mayne (1998) suggested a first theoretical approach to evaluate the behavior of pore pressure with a wide range of normally to heavily over consolidated soils. According to evidence, excess pore pressure dissipated with decreasing monotonically in normally and lightly over consolidated clays at the filter location on the cone face (u_1), behind the cone tip (u_2) and behind the sleeve friction (u_3). However, excess pore pressure of heavily over consolidated clays firstly was increasing and then decreasing with time at the filter location on the behind the cone tip (u_2) and behind the sleeve friction (u_3). In addition, excess pore pressure consisted two separate effects;

normal stress ($\Delta\sigma_{oct}$) which was became by displacement in soil and fluid during the cone penetration and shear stress ($\Delta\delta_{oct}$) which was became by shear displacement of soil adjacent to the cone, and it was observed that the shear stress significantly affected the dissipation of pore pressure at u_2 position of the cone. The measurement taken from u_2 position due to correcting the cone resistance was important. Thus, the shear induced dilatory response which causes negative excess pore pressure should be taken into account to calculate the correct t_{50} values. They proposed a hybrid analytical solution with using cavity expansion theory and critical state soil mechanics. Their solution could be used to evaluated for many sites from soft to stiff clays which was consistent with laboratory measurements. Laboratory and in-situ works should be continued to verify.

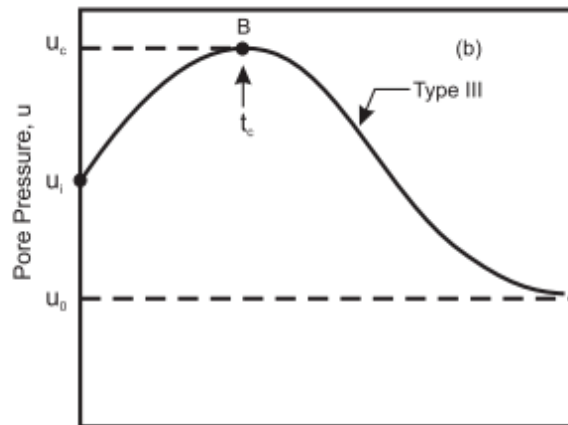
Sully et al. (1999) studied to estimate c_h values from different types of the excess pore pressure dissipation and classified these different types. They suggested the reasons of initial distribution of the dissipation of excess pore pressure as;

- 1) Poor saturation or poor measurement system
- 2) Redistribution of pore pressure from the cone tip to the behind the cone tip
- 3) Maximum pore pressure located away from the shaft in over consolidated soils

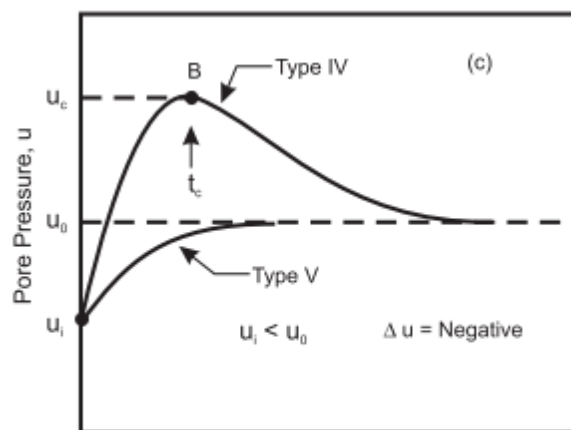
First and third ideas above proposed by authors were contradictory in some cases of the dissipation. Therefore, for second idea, characteristic distributions of pore pressure were examined with respect to its hydrostatic pressure to determine the behavior of the dissipation from normally to over consolidated soils. As a consequence, five types of the dissipation were suggested depending on soil characteristics, filter location and OCR. Type I was related to normally consolidated soils and other types of dissipations as Type II, Type III, Type IV and Type V were for over consolidated soils as it can be seen in Figure 2.11 a, b, and c.



Time, t



Time, t



Time, t

Figure 2.11. The dissipation of pore pressure in OC soils a) Type II b) Type III c) Type IV and Type V (Source: Sully et. al., 1999)

Available theories could not be enough to evaluate these curves to understand c_h values of soils. They proposed the method of shifting to the maximum pore pressure value either on the cone tip or behind the cone tip in logarithmic time space. Thus, the maximum pore pressure value was taken the peak and its time was a new zero time of the dissipation record for the behind the cone tip location. Therefore, a new form of normalized excess pressure graph could be replotted with respect to the peak value because of unloading and redistribution effects. Theoretically it can be acceptable, but the initial pore pressure distribution cannot be taken into account in this way.

Chai et al. (2012a) proposed an empirical formula based on numerical analyses which was applied on numerically simulated non-standard dissipation curves and some field tests. There was no easy-to-use formula to determine c_h values of non-standard dissipation curves. In this study, it was aimed to investigate the influence of the initial distribution around the cone on the dissipation, and find the correct t_{50} values from these curves with considering the redistribution of excess pore pressure. The reason of the behavior of pore pressure at the behind the cone was suggested volumetric expansion by the partial unloading effect when a soil element moved from the face to the shoulder of the cone during the cone penetration by Chai et al. (2012a). During the numerical investigation, it was seen that the larger dilatancy angle of soil caused the more negative excess pore pressure at the behind of the cone. Even if there were some assumptions in the analysis, shortcomings could be tolerable because the initial excess pore pressure distribution was mainly investigated. As a result of the study in Figure 2.12 that was used the same c_h value in all numerical simulation, it was observed that t_{50} values of non-standard dissipation curves was longer than that are t_{50} values of monotonically decreased curves. Therefore, c_h values obtained from non-standard dissipation curves were lower than that were c_h values of monotonically decreased curves. Based on the numerical simulation, the empirical equation proposed by Chai et al. (2012a) was;

$$t_{50c} = \frac{t_{50}}{1 + 18.5 \left(\frac{t_{u,\max}}{t_{50}} \right)^{0.67} \left(\frac{I_r}{200} \right)^{0.3}} \quad (2.4)$$

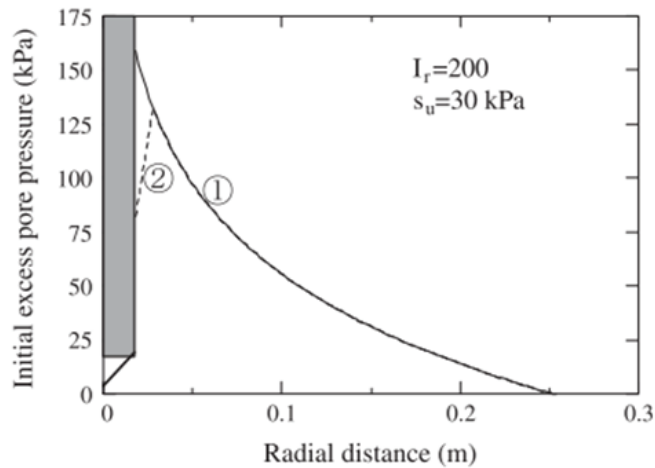
where;

$t_{u,\max}$ = time for measured pore pressure to reach its maximum value

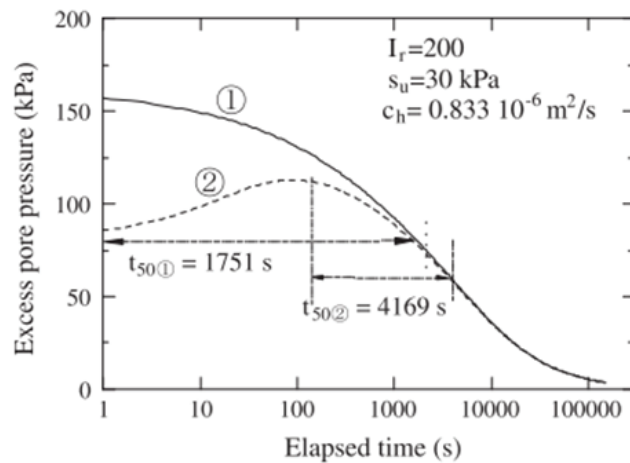
t_{50} = observed time difference between maximum and 50% of the maximum pore pressure

t_{50c} = corrected time for 50% pore pressure dissipation

c_h values could be obtained for non-standard dissipation curves using this equation. Therefore, t_{50c} values could be substituted into the method of Teh and Houlsby (1991) which was developed for monotonically decreased dissipation curves.



(a) Initial excess pore pressure distribution



(b) Dissipation curves

Figure 2.12. a) Initial excess pore pressure distribution b) dissipation curves

(Source: Chai et al., 2012a)

Dejong and Randolph (2012) proposed a new equation to find t_{50} values of the non-standard dissipation curve. The reason of initial distribution of excess pore pressure in intermediate soils was the partial drainage condition according to Dejong and Randolph (2012). However, this method was consistent using instead of the method of Teh and

Houlsby (1991) than that was when t_{50} values were less than 100 sec. The formula which was developed as the modification of the method of Teh and Houlsby (1991) is;

$$t_{50} = \frac{\sqrt{I_r}}{c_h} [78 + 0.25c_h^{1.2}] \quad (2.5)$$

The inferences point out that if t_{50} values were less than 100 sec, the partial drainage existed in the intermediate soil at standard penetration rate was 2 cm/sec.

Ha et al. (2014) developed an interpretation method for c_h values in over consolidated soils according to dilatory response using numerical simulation results. They mainly based on the reason of the initial excess pore pressure distribution was OCR values of the soil besides the values I_r and s_u . This method provided the evaluation of c_h values without the rigidity index (I_r). According to the numerical simulation, three indices were used to determine the time factor (T) of the dilatory behavior that were T_{max} , T_{50} and degree of excess pore pressure increment (DEPPI). However, T_{50} was selected to examine DEPPI which was defined as the ratio of maximum excess pore pressure to initial excess pore pressure ($\Delta u_{2max}/\Delta u_{2i}$) and T_{50} was the time factor of t_{50} values indicated the time of the half of initial excess pore pressure ($\Delta u_{2i} * 0.5$). As a result of that, the modified time factor (T_{50}^d) was obtained based on the linear correlation between T_{50} and DEPPI and c_h values could be unclear found in this way.

$$T_{50}^d = \frac{c_h t_{50}}{r_o^2 (r_p / r_o)^{1.25}} \quad (2.6)$$

where;

r_p = plastic zone

r_o = cone radius

T_{50}^d = modified time factor

$$T_{50}^d = 0.52DEPPI - 0.25 \quad (2.7)$$

where;

DEPPI = degree of excess pore pressure increment

$$r_p / r_o = [0.24(T_{50} / T_{\max}) - 0.86 - 0.24(t_{50} / t_{\max}) - 0.86] \quad (2.8)$$

where;

T_{\max} = time factor for $\Delta u_{2\max}$

T_{50} = time factor for $\Delta u_{2i} * 0.5$

Mahmoodzadeh et al. (2014) studied to estimate the operative consolidation coefficient from the pore pressure dissipation test using numerically simulated cone penetration results and after compare these c_h values to that obtained from the oedometer or Rowe cell consolidation test. OCR and I_r variables were major reasons of initial excess pore pressure during the dissipation as in Ha et al. (2014). During this study, the estimation of c_h values was made using the permeability coefficient (k) not the dissipation time of non-standard curves. And non-standard dissipation curves were obtained using heavily over consolidated soils which had maximum 5 of OCR value. It was not enough to determine the dilatory behavior of the soil.

2.4.2. Direct Push Permeability Test (DPPT)

In literature, many researchers used k values to examine c_h values of different drainage conditions of soils as Schneider et al. (2007), Yi et al. (2012), Huang (2015) and Cecceto and Simonini (2017). They majorly obtained k parameter using either laboratory studies such as the oedometer test, Rowe cell test or empirical relations with the other soil parameter based on in situ observations. Recently, an independent method had been developed to directly measure k values from the field. It was called as Direct Push Permeability Test (DPPT) proposed by Lee et al. (2008) and the permeameter can be seen in Figure 2.13.

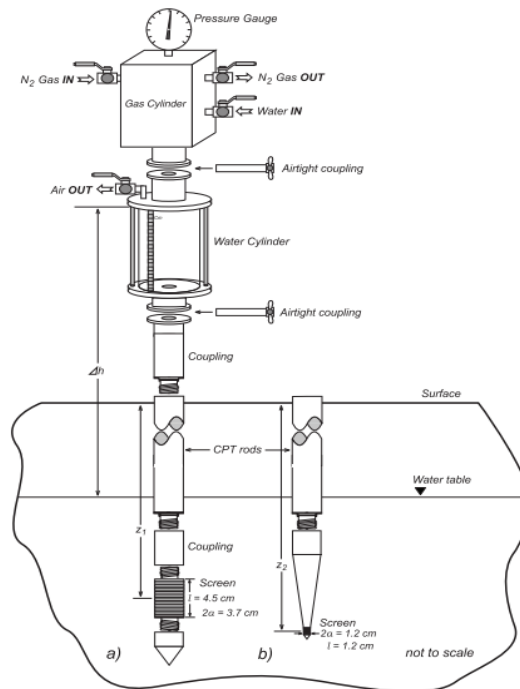


Figure 2.13 The permeameter test equipment with two different diameter probe tips a) $2a = 3.7$ cm b) $2a = 1.2$ cm

They aimed to obtain a correlation between CPTu indices and the hydraulic conductivity from DPPT. There was a procedure in Lee et al. (2008) how to use the permeameter. DPPT involved pressurizing water column with compressed nitrogen gas into the soil and measuring the change in discharge from the water column. The flow rate of water as Q , was manually measured as a volume discharge over a measured time. The equation of hydraulic conductivity based on Darcy's Law is;

$$k = \frac{Q}{4\pi\Delta h a_s} \quad (2.9)$$

where;

a_s = effective radius of the spherical injection zone

Δh = applied excess head

Q = measured volumetric flow rate

Therefore, c_h values of soils could be determined using this equation;

$$c_h = \frac{k_h}{m_v \gamma_w} \quad (2.10)$$

where;

m_v = compressibility of soil

γ_w = unit weight of water

DPPT was not suitable to understand k values of undrained penetration. Both Lee et al (2008) and Ecemis and Karaman (2014) mentioned the undrained response in hydraulic conductivity measurement. According to the relation between CPTu and DPPT proposed by Lee et al. (2008), the hydraulic conductivity could be defined using the results of CPTu induced the steady pressure distribution. However, the generated pressure had to be partially drained because of the strength parameter. Ecemis and Karaman (2014) supported this idea with respect to their DPPT results. They suggested that undrained impermeable layers were strongly influenced by the neighboring zones. DPPT was used to examine k values of clean sand and silty sand layers in their investigation. Therefore, we need the other method (PPDT) to obtain c_h value for undrained layers.

2.5. Relative Density Values Using SPT-(N)₍₆₀₎

Standard penetration test (SPT) is widely used to determine in-situ properties of granular soils. It is known that the penetration resistance of SPT is affected from fines content in soils and sands with fines have smaller SPT-N values than clean sands. Therefore, many researchers studied about the relation between SPT-N value and the relative density (D_r) which was generally mentioned related to maximum and minimum void ratio of soils. Meyerhof (1956), Skempton (1986), Kulhawy and Mayne (1990), Kibria and Masood (1998), Cubrinovski and Ishihara (1999) and Mujtaba et al. (2018) were some of these researchers.

The method of Meyerhof (1956) is a well-known relation that the penetration resistance was increased with the square of the relative density. The equation of the penetration resistance which be in the direct proportion with the effective overburden pressure of clean sand is;

$$N_{60} = \left(17 + 24 \frac{\sigma_v'}{98} \right) D_r^2 \quad (2.11)$$

where;

σ_v' = effective overburden stress

N_{60} = corrected SPT blow count for field procedure

Skempton (1986) developed the equation of Meyerhof (1956) according to some parameters based on over consolidation ratio, aging and grain size of sands. Kulhawy and Mayne (1990) correlated the relative density with the corrected SPT-N blow count according to the field conditions and overburden stress ($N_{1(60)}$) by using the same parameters as Skempton (1986) as were over consolidation, aging and grain size of sands. The equation of Kulhawy and Mayne (1990) is;

$$D_r = \sqrt{\frac{N_{1(60)}}{C_P C_A C_{OCR}}} \quad (2.12)$$

where;

$N_{1(60)}$ = corrected SPT blow count for field procedure and overburden stress

C_P = factor for grain size

C_A = factor for aging

C_{OCR} = factor for over-consolidation

Kibria and Masood (1998) proposed the following relation between the corrected SPT-N blow counts and the relative density for fine and silty sands;

$$D_r = 16.5 \sqrt{N_{1(60)}} \quad (2.13)$$

Cubrinovski and Ishihara (1999) showed that the method of Meyerhof (1956) caused to underestimate the relative density of silty sands and fine sands. There was a clear tendency that the mean grain size (D_{50}) parameter affected on the change in constant parameters of the method of Meyerhof (1956). They proposed a new equation;

$$D_r(\%) = \sqrt{\frac{N_F (0.23 + \frac{0.06}{D_{50}})^{1.7}}{9} \left(\frac{98}{\sigma_v'}\right)^{1/2} * 100} \quad (2.14)$$

where;

N_F = measured SPT blow count

D_{50} = mean grain size

Mujtaba et al. (2018) used Statistical Package for the Social Sciences (SPSS) software to develop the correlation of the relative density depending on many parameters such as the corrected SPT-N blow count (N_{60}), void ratio range ($e_{max}-e_{min}$), the effective overburden stress (σ_v') and in-situ dry density (γ_{df}). As a result of the correlation analysis, N_{60} and σ_v' parameters had significant effects on the relative density of sands. The model finally obtained was;

$$D_r(\%) = 1.96N_{60} - 19.2 \left(\frac{P_a}{\sigma_v'}\right)^{0.23} + 29.2 \quad (2.15)$$

where;

σ_{vo}' = effective overburden stress

P_a = atmospheric pressure

CHAPTER 3

INTERPRETATION OF FIELD TEST RESULTS

3.1. Introduction

Drainage conditions of soils extraordinarily affect the cone penetration resistance and excess pore pressure during the cone penetration into the soils. Drainage conditions should be carefully defined for silty sands according to relative density because it is observed that if the cone penetration is performed with respect to the standard penetration rate of 2 cm/sec, silty sands do not precisely show as properties of sand or clay soils. Properties of silty sands are called partially drained during the cone penetration under standard conditions. However, the limits of the partially drained behavior of silty sands have not been clearly defined yet.

This chapter mentions which interpretation methods should be applied to field test results to determine the behavior of partially drained soil. Four field tests were conducted on the northern side of the Izmir Gulf as standard penetration test (SPT), piezocone penetration test (CPTu), pore pressure dissipation test (PPDT), and direct push permeability test (DPPT). Then, the test results were interpreted to get the relationship between normalized cone resistance (q_{c1N}) or normalized excess pore pressure ($\Delta u/\sigma_{v0}'$) and non-dimension penetration rate (T) considering the relative density (D_r) of silty sands and clean sands.

3.2. Evaluation of Field Test Results

3.2.1. Standard Penetration Test (SPT) Result – D_r

SPT is one of the well-known testing methods to determine soil properties. Because it is universally applied and simple. To briefly mention the procedure of SPT, the numbers of blows of the hammer are measured for each three 15 cm (45 cm) depth intervals as seen in Figure 3.1. The last two 15 cm (30 cm) are generally added to find the

standard penetration number (SPT-N) defined in ASTM D-1586. Additionally, SPT provides to take a soil sample from the field. SPT-N values can be standardized by 60% of the potential energy according to the definition in the standard. Therefore, SPT-N values are corrected by the 60% average energy efficiency for the hammer (C_E), correction for borehole diameter (C_B), sampler correction (C_S), and correction for rod length (C_R) that are called N_{60} values (Das, 2007).



Figure 3.1. The photo of SPT test truck and SPT tests application in the region between Cigli and Karsiyaka taken by Ecemis et al.

SPT was performed at twenty different locations in 2013 by Ecemis et al. The locations of the tests were given on the Northern coast of the Izmir Gulf. A total of 173 disturbed samples were collected. After that, laboratory tests were conducted to determine such soil index parameters as grain size, Atterberg limits, specific gravity, and maximum and minimum void ratio. The soil type of samples obtained from the boreholes was mainly classified as poorly graded clean sand (SP) to silty sand (SM) and clayey sand (SC), with fines content ranging from 1% to 50% according to Figure 3.2. This classification was determined by using the Unified Soil Classification System (USCS) in ASTM D-2487.

Nonetheless, a small number of interbedded layers of silt and clay were encountered throughout the depth in the field.

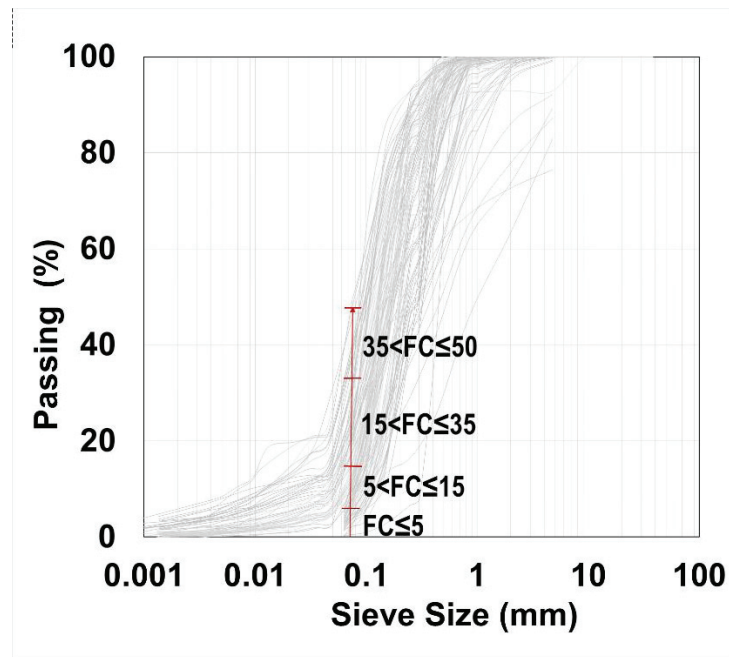


Figure 3.2. Grain size distribution graph of samples collected from field

Table 3.1. Maximum and minimum C_u , D_{50} , and FC values and number of samples related to the amount of FC

	MAXIMUM	MINIMUM
C_u	22.14	1.17
D_{50}	0.55	0.08
FC	49.44	0.5
	Number of samples of the relevant fines content	
FC < 5%	25	
5% < FC < 15%	81	
15% < FC < 35%	49	
35% < FC < 50%	19	

FC: fines content of soil; C_u : uniformity coefficient of soil; D_{50} : mean grain size of soil

The fines of 92 samples were non-plastic, and the others were low plastic, ranging from 0.3 to 40 according to hydrometer test results. Table 3.1 showed that 25 disturbed samples were collected with less than 5 % fines content (FC), 81 disturbed samples were collected between 5% and 15% FC, 49 disturbed samples were collected between 15% and 35% FC, and 19 disturbed samples were collected between 35% and 50% FC. The mean grain size (D_{50}) of the whole collected samples was in the range of 0.08 mm to 0.55 mm, the uniformity coefficient (C_u) was in the range of 1.17 to 22.14.

Relative density (D_r) is an essential stiffness parameter to understand the normalized cone penetration resistance (q_{c1N}) of fine-grain sands. Because q_{c1N} has different behavior under different densification and fines content of the soils. In this study, N_{60} values were evaluated to calculate the D_r values of silty sands and sands at each depth where SPT was conducted. The N_{60} values can be found in Karaman's (2013) MS Thesis and Ecemis (2014). D_r calculations were made using N_{60} had given in Appendix A. Mujtaba et al.'s (2018) method was applied to determine D_r values; the latest method indicated the relationship between D_r and N_{60} . After that, D_r values obtained using the method of Mujtaba et al. (2018) were compared with those of Cubrinovski and Ishihara (1999).

N_{60} values were observed as between 2 and 28 that were corrected blow count of SPT. Some correlations were mentioned in Chapter 2 to determine the D_r of soil by using N_{60} values. The latest method related to the interpretations of D_r proposed by Mujtaba et al. (2018) was;

$$D_r(\%) = 1.96N_{60} - 19.2 \left(\frac{P_a}{\sigma_v} \right)^{0.23} + 29.2 \quad (3.1)$$

D_r values of soil strata was determined between 9 (very loose) and 67 (medium dense) using the method given by Mujtaba et al. (2018). In literature, Meyerhof (1956), Skempton (1986), Kulhawy and Mayne (1990), Kibria and Masood (1998), and Cubrinovski and Ishihara (1999) had proposed relationships between N_{60} and D_r . The most recent method before Mujtaba et al. (2018) belonged to Cubrinovski and Ishihara (1999) and comparison was made between them. As a result of that produced by the method of Cubrinovski and Ishihara (1999), D_r was found bigger than 100% that was

impossible for an ideal densified soil strata. D_r values were obtained between 198% and 38% using measured SPT-N values according to Cubrinovski and Ishihara (1999).

The reason for this result can be that Cubrinovski and Ishihara (1999) studied the mean grain size (D_{50}) effect of silty sand on D_r values using the relation between the parameter of $(e_{\max}-e_{\min})$ and D_{50} values. However, the parameter of $(e_{\max}-e_{\min})$ did not support the soil classification according to their relation. For instance, the depth of silty sand as SM with respect to the USGS soil classification chart had given 1.02 of the parameter of $(e_{\max}-e_{\min})$. However, the chart of Cubrinovski and Ishihara (1999) said that the range must be between 0.6 and 0.7. On the other hand, Mujtaba et al. (2018) proposed the effective stresses of silty sands more affected D_r values. Experimental results calculated from undisturbed field samples fitted the predicted data obtained from the method of Mujtaba et al. (2018), and the standard error of estimate (SEE) was found within + %10. So that, it was thought that the method of Mujtaba et al. (2018) was more consistent even if dense soil strata were not obtained in twenty SPT locations.

3.2.2. Piezocone Penetration Test (CPTu) Result – q_{c1N} and $\Delta u/\sigma_{v0}'$

CPTu is mainly used without taking the field sample to determine soil properties such as soil behavior type, coefficient of consolidation, OCR, relative density, undrained shear strength, etc. In this study, the results of CPTu used to evaluate q_{c1N} and $\Delta u/\sigma_{v0}'$ were conducted at the constant speed 2 cm/sec and constant diameter of the cone 3.57 cm according to ASTM D5778 and ASTM D6067. CPTu parameters were taken for 1 cm of each penetration depth. The results of CPTu can be found in Karaman's (2013) MS Thesis and Ecemis (2014), such as SPT results. At this site, the water table was varying between 1.06 m and 3.4 m, and the lowest depth performed CPTu was 6 m. Therefore, it indicated that the whole testing area was saturated. Nevertheless, it was clear that the excess pore pressure generated around the cone would affect the cone resistance during the penetration with respect to Lunne et al. (1997).

Generally, the cone resistance (q_c), friction resistance (f_s), and pore pressure (at the u_2 position) are measured during the cone penetration. Pore water pressure can be determined at three different locations on the cone: 1) the cone tip referred to as u_1 2) behind the cone tip referred to as u_2 3) behind the friction sleeve referred to as u_3 . Baligh et al. (1981) defined that pore water pressure at the cone tip (u_1) did not affect the cone

resistance. And also, Randolph and Hope (2004) said that the u_1 position was better for identifying soil type while the u_2 position was good at deducing c_h values. Therefore, pore water pressure was measured on the behind of the cone (u_2).

The cone resistance was corrected according to overburden stress by using the relationship given by Youd et al. (2001).

$$q_{c1N} = C_q \left(\frac{q_c}{P_a} \right) \quad (3.2)$$

$$C_q = \left(\frac{P_a}{\sigma_{v0}} \right)^m \quad (3.3)$$

where;

σ_{v0}' = initial effective vertical stress

P_a = atmospheric pressure with the same unit as initial effective vertical stress, 101.33 kPa

$m = 0,784 - 0,521D_r$, was applied for the C_q value proposed by Boulanger (2003).

In this instance, D_r values were found using the equation (3.1) provided to determine m values. Therefore, it was indirectly observed that the effect of D_r of silty sand on q_{c1N} . It can be found how D_r values were obtained in section 3.2.1, Standard Penetration Rate (SPT).

C_q value cannot exceed 1.7. Therefore, if the result of the C_q calculation had been over 1.7, it was taken as 1.7.

Based on the normalization of the cone penetration outcomes proposed by Wroth (1984), the pore pressure was normalized as $\Delta u/\sigma_{v0}'$ using overburden stress as mentioned in Dejong and Randolph (2012), and Schneider et al. (2007).

$$\frac{\Delta u}{\sigma_{v0}'} = B_q Q_t \quad (3.4)$$

$$B_q = \frac{u_2 - u_0}{q_c - \sigma_{v0}} \quad (3.5)$$

$$Q_t = \frac{q_c - \sigma_{v0}}{\sigma_{v0}} \quad (3.6)$$

where;

B_q = dimensionless pore pressure ratio

Q_t = dimensionless cone resistance

3.2.3. Pore Pressure Dissipation Test (PPDT) Result – c_h

Pore Pressure Dissipation Test (PPDT) is the valid method with respect to its time relationship to determine the horizontal coefficient of consolidation of soil (c_h) because of the negligible effect of the vertical coefficient of consolidation (c_v) (Teh and Houlsby, 1991). This test provides the direct way to examine c_h according to the dissipation time of 50% excess pore pressure (t_{50}) induced around the cone during the penetration as long as the dissipation of excess pore pressure has given a good result. For example, PPDT was conducted at a depth of 8.5 m in the SC16 borehole. The water table was at 2.81 m in this borehole. When the piezocone penetration was stopped at a depth of 8.5 m, the time of pore pressure dissipation was started to measure. Once the excess pore pressure was stable, the dissipation measurement was stopped, as seen in Figure 3.3. In this instance, it could be clearly observed 50% of pore pressure dissipation from the graph. All other curves from which t_{50} values had been calculated were given in Appendix B. The point which is on the x-axes of the curve indicated t_{50} . The dissipation time depends on soil index parameters such as permeability, consolidation coefficient, and soil compressibility.

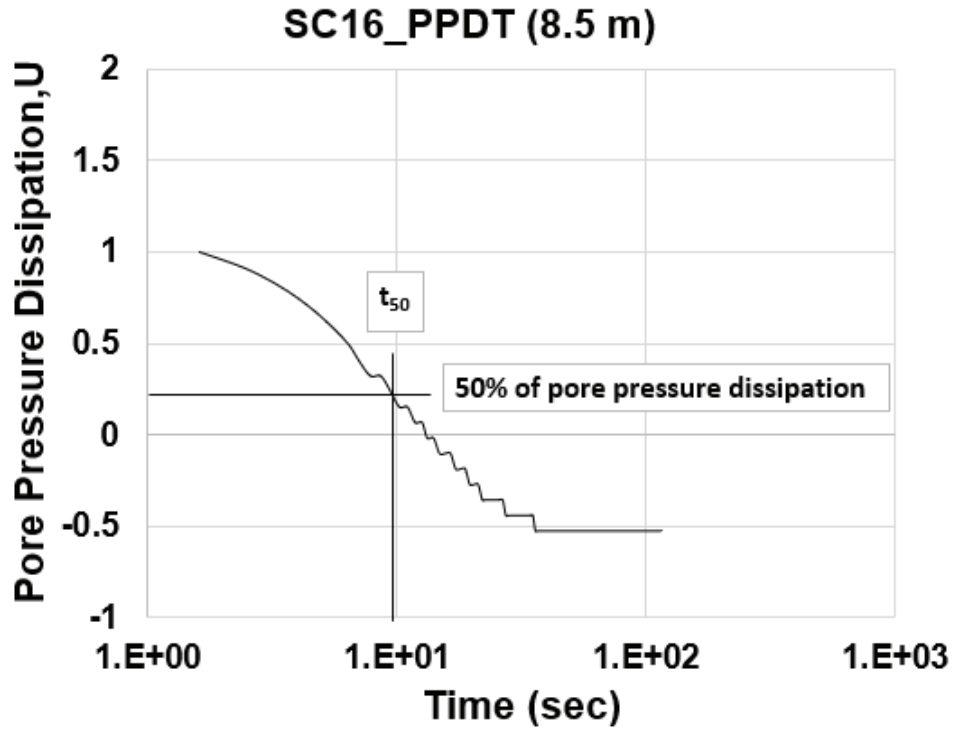


Figure 3.3. An example curve of how to get t_{50} from dissipation test graphs (SC16, 8.5 m)

In this study, t_{50} was preferred to obtain c_h of soils as mentioned above directly, and some researchers investigated the effects of t_{50} on c_h under different drainage conditions, such as Burns and Mayne (1998), Sully et al. (1999), Chai et al. (2012), Dejong and Randolph (2012). Investigations about the dissipation analysis were detailly mentioned in section 2.4.1.

First of all, excess pore pressure values were normalized to examine the dissipation rate with respect to the hydrostatic pressure of the soil in the field. Therefore, it was important to know the definite water level when excess pore pressure was measured.

$$U_i = \frac{u_{2_i} - u_0}{u_{2_1} - u_0} \quad (3.7)$$

where;

u_0 = hydrostatic pressure at the stopped depth

u_{2_i} = measured pore pressure at i^{th} time

u_{2_1} = measured pore pressure at $t = 0$

This method was used to interpret the dissipation of excess pore pressure. Because dissipation curves with measured pore pressure at behind the cone tip (u_2) needed to classify five characteristic types according to the hydrostatic pressure, which belongs to the measurement depth. For example, if the pore pressure dissipation begins under the hydrostatic pressure and then increases to the hydrostatic pressure, they call Type V. (Sully et al. 1999). Apart from these types of dissipation, the normalized pore pressure graph was plotted to time instead of the measured pore pressure to correctly examine t_{50} of pore pressure dissipation, as shown in Figure 3.4.

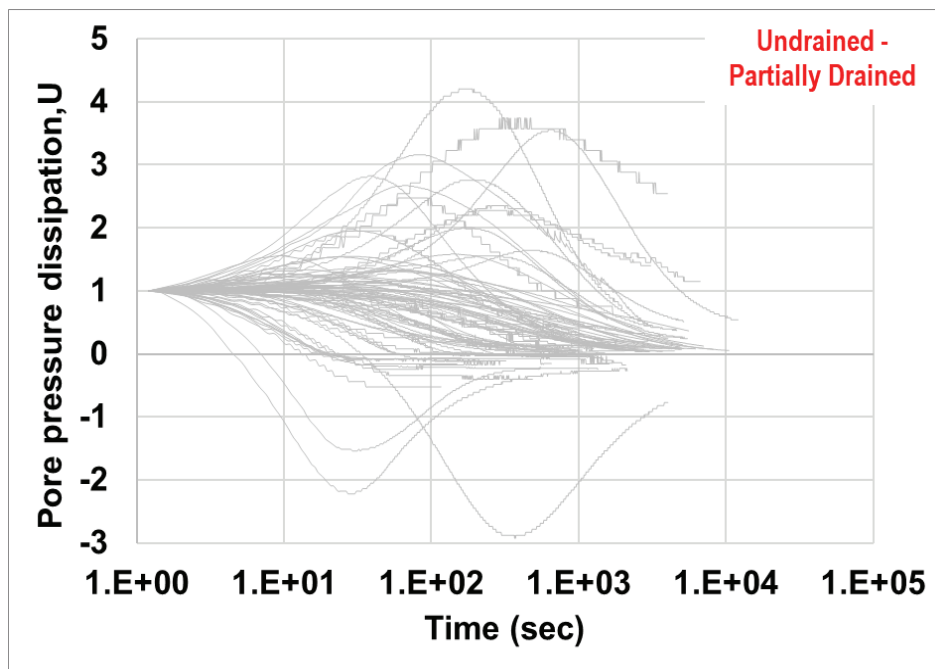


Figure 3.4. Undrained - partially drained normalized pore pressure dissipation curves that were found from 84 dissipation curves

It can be seen different types of dissipation curves in Figure 3.4. Even if normalized dissipation curves decreased the classification number and made it easy to investigate, they could not be totally avoided to classify. However, normalized dissipation curves allowed us to create our types without using the hydrostatic pressure, as they can be viewed later in this section.

There were some inferences about these types in dissipation graphs, such as over consolidation ratio for clays or densification for sands and measurement location on the cone. (Burns and Mayne, 1998, Sully et al., 1999). The measured pore pressure was behind the cone tip (u_2) during the whole test procedure. In case of that, these differences were not related to the location of the measurement. Nevertheless, it was known that the

finer content of measured samples was not above 50% ($FC < 50$) according to samples taken from SPT. Until now, heavily over consolidated clay samples were mainly examined for types in pore pressure dissipation, as detailedly mentioned in section 2.4.1. However, it was seen in this investigation that PPDT could give consistent results, and changes in dissipation curves could also be observed for silty sands or clayey sands. For this reason, the correct interpretation of the dissipation of pore pressure was investigated throughout the study under partially and undrained penetration conditions referring to the behavior of clay.

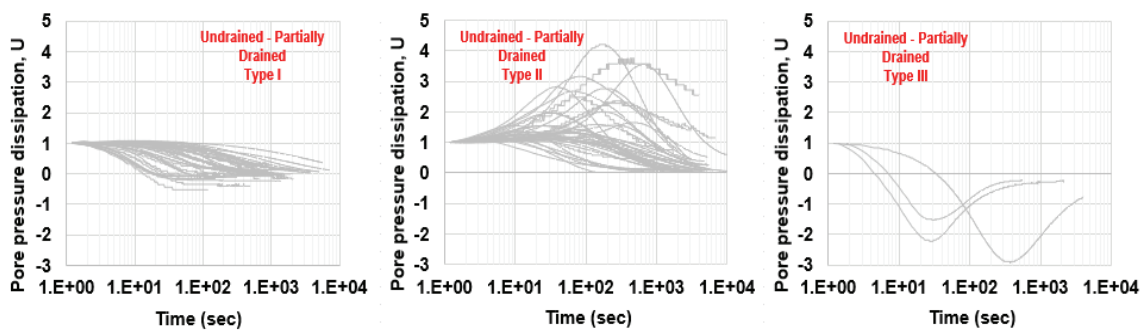


Figure 3.5. a) Type I b) Type II and c) Type III undrained-partially drained dissipation curves of silty sands

Three types of pore pressure dissipation curves; Type I, Type II and Type III were observed and plotted in Fig 3.5 as Sully et al. (1999) do. In Type I curves of pore pressure dissipation, normalized excess pore pressure monotonically decreased with time. However, in Type II curves of pore pressure dissipation, which is generally called non-standard dissipation, normalized excess pore pressure first increased and after decreased in the following time. Type II curves are well-known related to heavily over consolidated clays because of dilatancy behavior. All solutions found until the late 1990s to determine c_h and t_{50} were valid for monotonically decreasing dissipation curves. Therefore, a different method was needed to examine t_{50} values for Type II dissipation of pore pressure. Burns and Mayne (1998), Sully et al. (1999), Chai et al. (2012a), Ha et al. (2014), Mahmoodzadeh et al. (2014) proposed some solutions which were based on respectively analytical, semi-analytical, empirical, and numerical methods for dissipation curves of pore pressure of clay soil. Dejong and Randolph (2012) also proposed a solution to examine t_{50} of pore pressure dissipation under partially drained penetration. However, it was suggested that this method was applicable when t_{50} was less than 100 sec. As a

result of the search to determine correct t_{50} , the method of Chai et al. (2012a) was selected to apply on Type II curves of pore pressure dissipation. Because they assumed the effect of initial distribution in Type II curves of excess pore pressure on the t_{50} values. The formulation which belonged to Chai et al. (2012a) is;

$$(t_{50})_c = \frac{t_{50}}{1 + 18.5 \left(\frac{t_{u,\max}}{t_{50}} \right)^{0.67} \left(\frac{I_r}{200} \right)^{0.3}} \quad (3.8)$$

where;

$t_{u,\max}$ = time for measured pore pressure to reach its maximum value

$(t_{50})_c$ = the corrected time for 50% pore pressure dissipation

I_r = rigidity index

I_r could be found by using this formula;

$$I_r = 15 \ln(q_c * 1000) + 39 \quad (3.9)$$

Three curves first decreased until their maximum negative values, then increased to zero excess pore pressure were obtained in Figure 3.5c called as Type III. These curves were evaluated as undrained – partially drained Type II curves because their dissipation behavior was similar to Type II curves. The same method of Chai et al. (2012a) was applied for three curves, too.

Other curves Type I did not need any correction method in Figure 3.5a because it was easy to determine the t_{50} of the dissipation, as an example in Figure 3.3. according to the method of Casagrande and Fadum (1940). The Casagrande and Fadum's (1940) method was based on logarithmic graphs to determine t_{50} for settlement. In this study, the half of excess pore pressure dissipation was examined to get t_{50} . After, t_{50} values were used to determine c_h values using the half time factor. Teh and Houlsby (1991) proposed a method with developing the existing method for c_h based on rigidity index (I_r).

$$c_h = \frac{T_{50} r^2 \sqrt{I_r}}{(t_{50})_c} \quad (3.10)$$

where;

T_{50} = time factor for 50% dissipation

r = radius of the cone

In general, drained type dissipation cannot be managed in most situations to predict the exact c_h value from drained to partially drained penetration. Therefore, DPPT was used to determine c_h values for silty soil layers where drained type dissipation was observed in the field.

3.2.4. Direct Push Permeability Test (DPPT) Result - c_h

DPPT provides to directly determine the permeability coefficient of soil (k) in the field. It has a simple procedure. First, water is pressurized from the aboveground reservoir with compressed nitrogen gas. And then, volume discharge is manually measured to find the flow speed through the depth defined in Lee et al. (2008). The equation of permeability is based on the spherical form of Darcy's Law proposed by Lee et al. (2008);

$$k = \frac{Q}{4\pi\Delta h a_s} \quad (3.11)$$

where;

a_s = effective radius of the spherical injection zone

Δh = applied excess head

Q = measured volumetric flow rate

In this study, a_s was calculated as 1.44 cm. This technique can be applied to partially drained and drained soil layers. It is hard to measure k value in undrained layers accurately, according to Ecemis and Karaman (2014), as detailedly mentioned in Chapter 2.4.2. In this aspect, if PPDT had given a reasonable curve for a layer of the borehole, DPPT could not be thought to calculate c_h of that layer. Most dissipation that belonged to drained penetration had given nonsense curves, and t_{50} could not be determined, as shown in Figure 3.6. On the other hand, some partially drained dissipation had t_{50} values which are less than 100 sec. It was difficult to obtain the correct t_{50} from these curves.

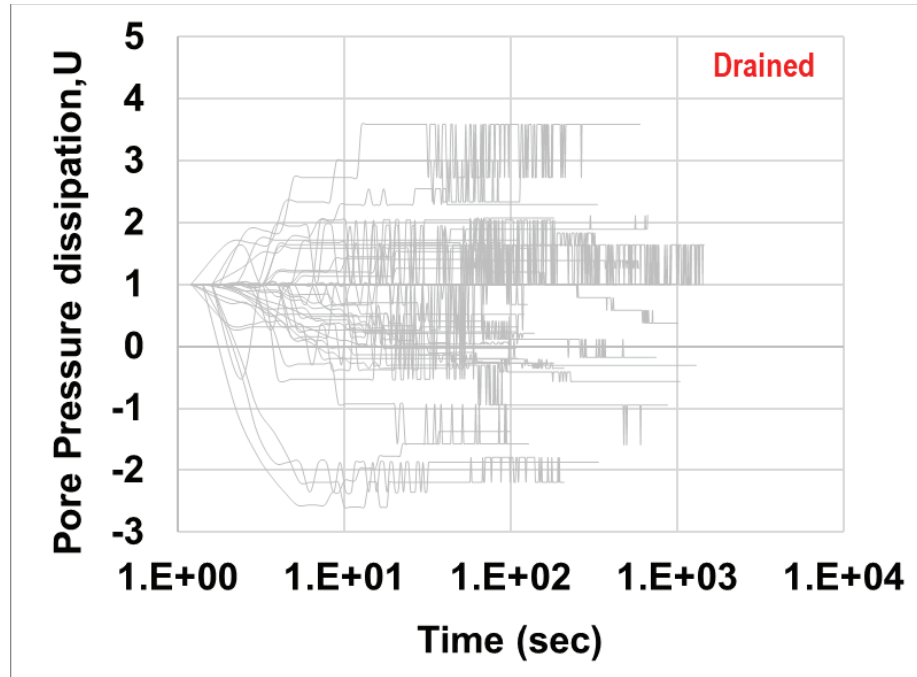


Figure 3.6. Drained excess pore pressure dissipation curves obtained from the field

Using the k values obtained from DPPT and, c_h parameters were calculated based on this equation;

$$c_h = \frac{k_h}{m_v \gamma_w} \quad (3.12)$$

where;

m_v = compressibility of soil

γ_w = unit weight of water

m_v was calculated according to the equation proposed by Robertson (2009) is based on CPT results.

$$m_v = \frac{1}{\alpha_m (q_t - \sigma_{v0})} \quad (3.13)$$

where;

q_t = total cone resistance

σ_{v0} = in-situ total vertical stress

For α_m ;

If $I_c > 2.2$ and $q_{c1N} < 14$, $\alpha_m = q_{c1N}$.

If $I_c > 2.2$ and $q_{c1N} > 14$, $\alpha_m = 14$.

If $I_c < 2.2$, $\alpha_m = 0.03[10^{(0.55I_c+1.68)}]$.

α_m was estimated using soil behavior type index (I_c).

$$I_c = [(3.47 - \log_{10} q_{c1N})^2 + (\log_{10} F + 1.22)^2]^{0.5} \quad (3.14)$$

I_c was modified by Robertson and Wride (1998) according to CPT results, and so it can be said that results of c_h using k values of DPPT are affected from q_{c1N} .

3.3. Non-Dimensional Penetration Rate

The drainage condition of the silty sand was estimated related to the coefficient of consolidation determined by using PPDT and DPPT. Non-dimensional penetration rate (T) parameter was introduced to demonstrate the degree of consolidation depends on such non-soil-property parameters as penetration rate (v) and cone diameter (d) according to Finnie and Randolph (1994), House et al. (2001), and Randolph and Hope (2004).

In this study, v and d values were constant, and therefore, T only depended on the c_h values. If the demarcation values of T are desired to determine between drained and undrained penetration, PPDT and DPPT should be interpreted carefully.

Until now, many T values were proposed for clayey soil, such as Schneider et al. (2007), Kim et al. (2008), Jaeger et al. (2010), and Oliveria et al. (2011). Nevertheless, there was limited estimation for silty sand, such as Thevanayagam and Ecemis (2008), Kumar and Bajju (2009), Kokusho (2012), and Huang (2015). In addition, it was plausible that the T value instead of only fines content was used for silty sands and sands proposed by Huang (2015). Because, even if fines content changed q_{c1N} by affecting $\Delta u/\sigma_{v0}'$ around the cone, the cone geometry (d) and penetration speed (v) affected q_{c1N} . Consequently, PPDT was generally applied for clayey soils because of the undrained behavior. But in this study, it was shown that PPDT was applicable for silty sands to propose a new T limit value of the drainage condition from partially drained to undrained compared to other investigations.

c_h values were interpreted from drained to partially drained penetration using permeability coefficient obtained from DPPT, which Lee et al. (2008) proposed as mentioned before in Chapter 2.4.2. Karaman (2014) also used this method to understand c_h values for drained penetration and combine T parameter for evaluating the relationship with the cone penetration resistance and excess pore pressure for the first time before.

CHAPTER 4

EFFECTS OF COEFFICIENT OF CONSOLIDATION and RELATIVE DENSITY ON q_{c1N} and $\Delta u/\sigma_{v0}'$

4.1. Introduction

The definition of Finnie and Randolph (1994), House et al. (2001), and Randolph and Hope (2004) clarify drainage conditions of soils as the non-dimensional penetration rate (T). This definition is applied to determine demarcation T values between drained and undrained conditions during the cone penetration. The coefficient of consolidation (c_h) is the most significant parameter if penetration rate (v) and cone diameter (d) are constant because of the definition of T value. The normalized cone resistance (q_{c1N}) of silty sands has not been well-defined with T values at the standard penetration rate (2 cm/sec). Therefore, q_{c1N} of silty sands needs to apply consistent interpretation methods and evaluate them according to the properties of silty sands. At the same time, the normalized excess pore pressure ($\Delta u/\sigma_{v0}'$) of silty sands has to be determined according to T values, because of the effect of $\Delta u/\sigma_{v0}'$ induced around the cone during penetration on q_{c1N} .

The relative density (D_r) is also a key stiffness parameter to define the behavior of $\Delta u/\sigma_{v0}'$ of silty sands. Then q_{c1N} of silty sands are affected from this relation between D_r and $\Delta u/\sigma_{v0}'$. Therefore, the effect of D_r on q_{c1N} and $\Delta u/\sigma_{v0}'$ of silty sands are needed to understand very well under different drainage conditions.

Firstly, PPDT and DPPT were used to estimate the c_h values of silty sands and clean sands in this study. In Chapter 3, we presented how c_h values were determined. As a consequence of this study, T values of partially drained conditions of silty sands vary between 10^{-3} and 10 according to the evaluation of c_h on q_{c1N} and $\Delta u/\sigma_{v0}'$.

Secondly, the effect of different D_r values was examined on q_{c1N} and $\Delta u/\sigma_{v0}'$. In this study, N_{60} values obtained from Standard Penetration Tests (SPT) were applied to determine D_r values, as mentioned in Chapter 3. Some inferences were observed from the graph q_{c1N} - T and $\Delta u/\sigma_{v0}'$ - T with respect to D_r even if dense soils were not obtained from

the field. The comparison for q_{c1N} and $\Delta u/\sigma_{v0}'$ was made between different densities, and it was observed that the change in q_{c1N} and $\Delta u/\sigma_{v0}'$ from loose to dense soils.

4.2. Effect of Consolidation Coefficient On q_{c1N} and $\Delta u/\sigma_{v0}'$

The drainage effect of silty soils plays a significant role in cone penetration resistance and excess pore water pressure. Primarily, it was observed that q_{c1N} and $\Delta u/\sigma_{v0}'$ were different for the same penetration rate if drainage conditions of soils around the cone were different, according to Thevanayagam and Ecmis (2008). The best way to understand the effect of drainage conditions with non-soil-property parameters was to determine non-dimensional parameter (T), which was used by Finnie and Randolph (1994), House et al. (2001), and Randolph and Hope (2004). Additionally, Huang (2015) proposed that T value instead of fines content (FC) was more appropriate to evaluate c_h during penetration. Hence, the T value was used to determine drained, partially drained, and undrained penetrations. This study estimated c_h values using PPDT and DPPT to determine T values of silty sands under different drainage conditions. It had been explained in detail how c_h and T values were found in Chapter 3.

Figure 4.1a, Figure 4.1b, and Figure 4.1c showed the distribution of q_{c1N} and $\Delta u/\sigma_{v0}'$ according to T value. Dot points referred that the values of q_{c1N} and $\Delta u/\sigma_{v0}'$ were displayed according to T values obtained from DPPT. Triangle points referred that q_{c1N} and $\Delta u/\sigma_{v0}'$ values were displayed according to T values obtained from PPDT. Figure 4.1a, Figure 4.1b, and Figure 4.1c were evaluated to determine the change in q_{c1N} and $\Delta u/\sigma_{v0}'$ with respect to different D_r ranges. Therefore, upper and lower limit lines were plotted as dashed lines for three different D_r ranges such as $10\% < D_r < 25\%$; $25\% < D_r < 45\%$; $45\% < D_r < 65\%$.

During this investigation, both q_{c1N} and $\Delta u/\sigma_{v0}'$ did not vary with T increase after 10. It was more apparent in graphs for medium dense to loose silty sands like Figure 4.1a and Figure 4.1b. When D_r was in the 45% and 65% range, q_{c1N} and $\Delta u/\sigma_{v0}'$ values were not obtained too much during the undrained penetration. However, more q_{c1N} values for undrained penetration were observed in the range of 45% and 65% of D_r from Karaman (2013), considering the same in-situ test results were used. Using the different methods to determine T values from PPDT can be a reason for the contradiction. However, the inference could be made that the non-dimensional penetration rate would not affect the

cone resistance when T would be bigger than 10 based on the $\Delta u/\sigma_{v0}'$ graph of Figure 4.1c.

On the other hand, the results of drained penetration were not matched with Karaman (2013) from medium dense to loose soils. In this investigation, the drained cone resistance did not change for all D_r values of soils when the normalized penetration rate is smaller than 10^{-3} , as seen from the graphs of q_{c1N} , especially Figure 4.1b and Figure 4.1c. If drained penetration results of Arık (2021) were added to q_{c1N} and $\Delta u/\sigma_{v0}'$ graphs of this study for all D_r ranges, the limit T value from drained to partially drained penetration could be proved as 10^{-3} . But, q_{c1N} values of loose silty sands under the drained penetration were not observed in Karaman (2013) despite the types of soils investigated in the field being known as poorly clean sands (SP) to silty sands (SM) or clayey sands (SC).

At the same time, c_h values obtained from PPDT were evidence to prove the demarcation value 10 of T . Figure 4.2 and Figure 4.3 were plotted as an example to compare the results of T values calculated using two different methods; Sully et al. (1999) and Chai et al. (2012a). These methods examined non-standard dissipation curves, which were mentioned in Chapter 3. c_h was found by using the method of Chai et al. (2012a) was bigger than c_h of that the method of Sully et al. (1999) according to the comparison between Sully et al. (1999) and Chai et al. (2012a) in Figure 4.2 and Figure 4.3 respectively. It indicated that the behavior of partially drained penetration was included much more in the method of Chai et al. (2012a). Therefore, it could be said that undrained penetration behavior was seen when T was bigger than nearly 10.

As a result of Figure 4.2 and Figure 4.3, the method of Chai et al. (2012a) provided to prove the limit value T was 10 from partially drained to undrained penetration because it reduced the difference between T values calculated using DPPT and those computed using PPDT. And so, it was understood that Chai et al. (2012a) was a proper method to obtain consistent results from undrained to partially drained penetration.

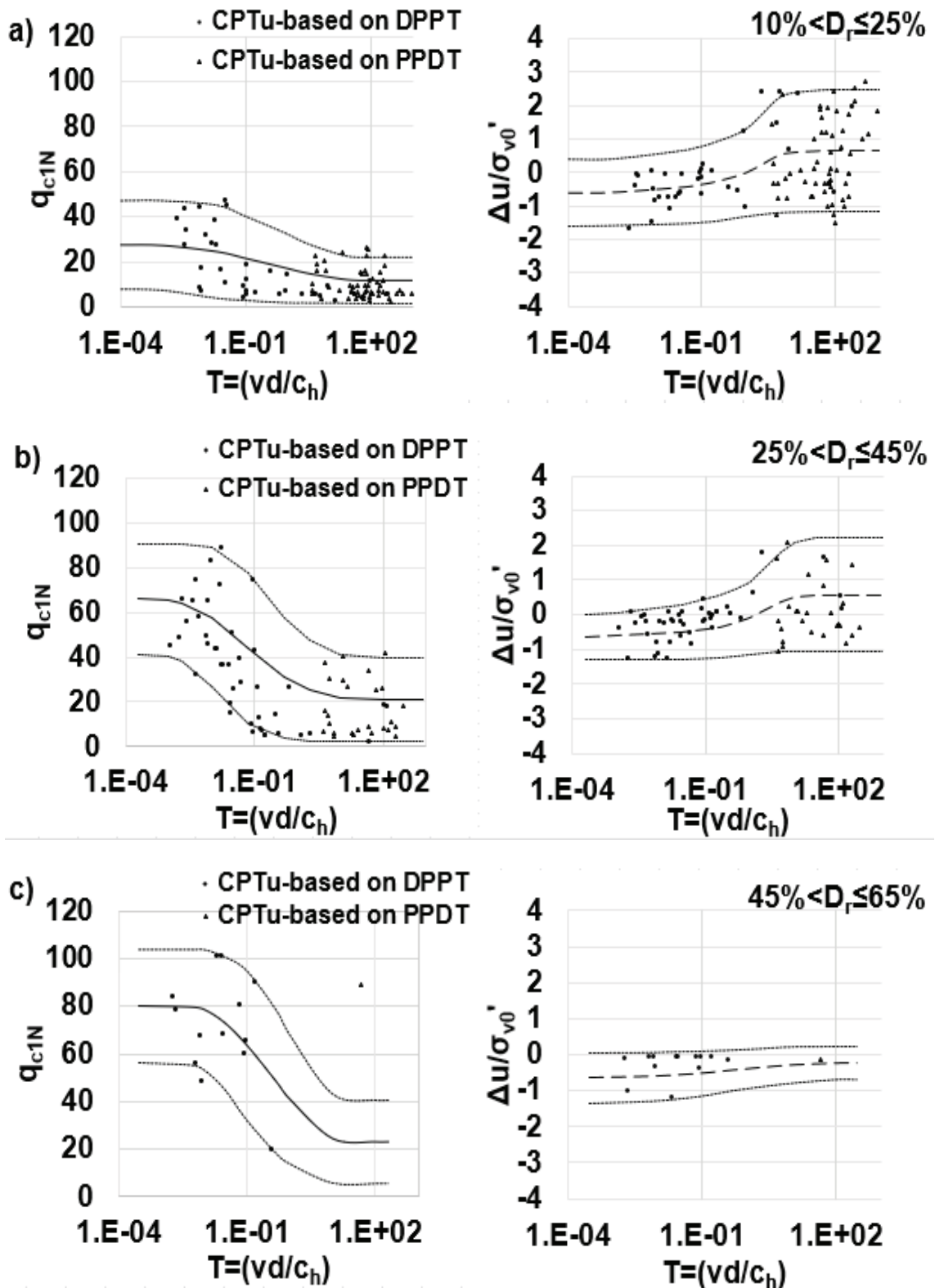


Figure 4.1. The graphs of q_{c1N} and $\Delta u/\sigma_{v0}$ values according to T values a) $10\% < D_r \leq 25\%$ b) $25\% < D_r \leq 45\%$ c) $45\% < D_r \leq 65\%$

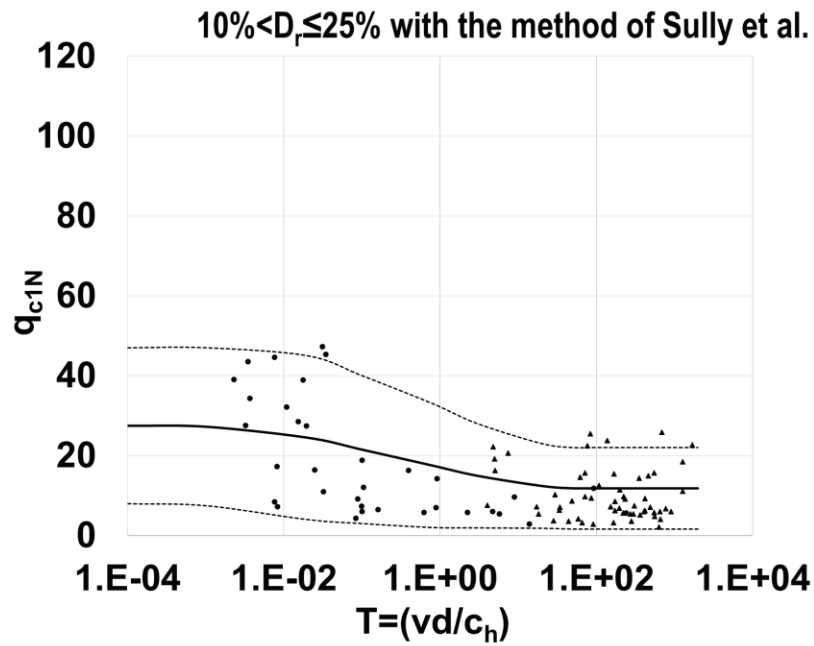


Figure 4.2. The graph of q_{c1N} according to the method of Sully et al. (1999)

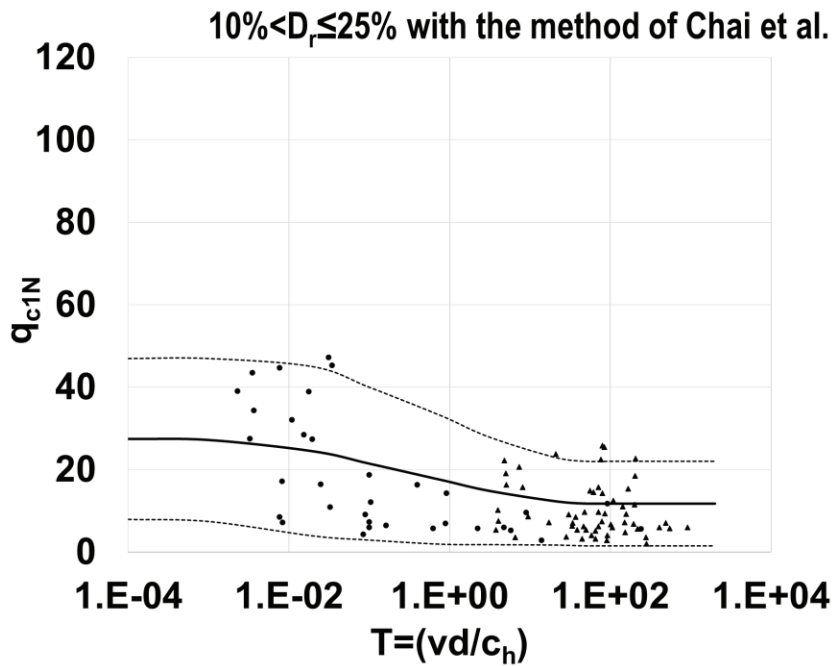


Figure 4.3. The graph of q_{c1N} according to the method of Chai et al. (2012a)

All data of the normalized cone resistance (q_{c1N}) and normalized excess pore pressure ($\Delta u/\sigma_{v0}'$) obtained from Figure 4.1 was plotted as a single graph according to non-dimensional penetration rate (T) as it can be seen in Figure 4.4. The behavior of q_{c1N} and $\Delta u/\sigma_{v0}'$ were examined according to the relative density (D_r) using the average values

of 55%, 35%, and 17%. Dashed lines indicated the change in $\Delta u/\sigma_{v0}'$ with respect to T values, and straight lines stated the change in q_{c1N} in Figure 4.4. Black lines of q_{c1N} and $\Delta u/\sigma_{v0}'$ were related to 55% D_r , red ones were related to 35% D_r and purple ones related to 17% D_r . Partially drained penetration of silty sands was in the range of T where q_{c1N} and $\Delta u/\sigma_{v0}'$ showed alterations.

The consequence of Figure 4.4 was that while the parameter of T was increasing, q_{c1N} decreased, and $\Delta u/\sigma_{v0}'$ increased depending on their D_r values. Mainly, a slight decrement in q_{c1N} was observed for loose soils when T values increased. For medium-dense soils, q_{c1N} significantly decreased when T values increased. On the other hand, $\Delta u/\sigma_{v0}'$ was inversely affected by the change in D_r values relative to q_{c1N} . In both cases, when T increased, $\Delta u/\sigma_{v0}'$ slightly increased for medium dense soil while $\Delta u/\sigma_{v0}'$ significantly increased for loose silty sands.

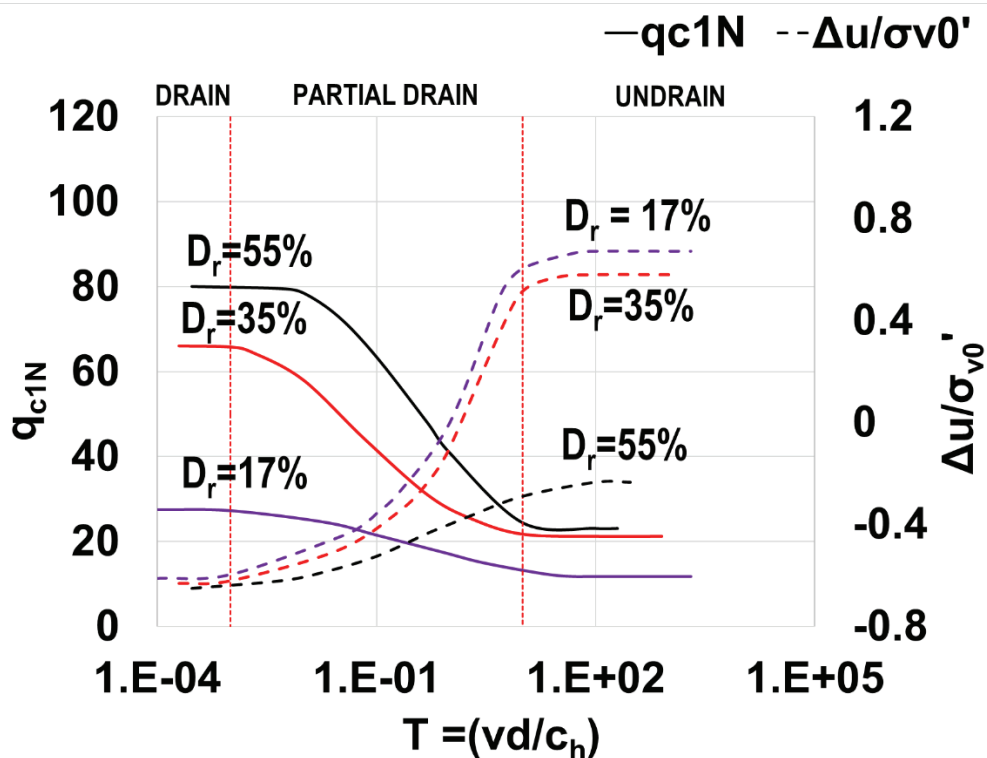


Figure 4.4. Trendlines of q_{c1N} and $\Delta u/\sigma_{v0}'$ at average relative densities of 17%, 35% and 55%

The demarcation T values for drained and undrained penetration obtained from the field study were compared to other investigations in the literature. There were some experimental researches about drainage effects during the cone penetration in silty sands for partially drained conditions (Kumar and Bajju, 2009; Kokusho et al. 2012; Karaman,

2013; Ecemis and Karaman, 2014; Huang, 2015) or clay for undrained conditions (Randolph and Hope, 2004, Schneider et al., 2007; Kim et al., 2008; Jaeger et al., 2010; Oliveira et al. 2011). And also, numerical simulations were used to understand the behavior of partially drained consolidation on the cone resistance (Thevanayagam and Ecemis, 2008; Yi et al., 2012; Cecceto and Simonini, 2017). Numerical investigations about the cone penetration in sand or clay soils were not paid attention to because of the research area of this study.

In the last years, a few experimental research were performed to determine limit values for T in silty sands. Kumar and Bajju (2009) studied the effect of variable penetration rate on the cone penetration resistance, as found in section 2.2. However, they did not get the T value from drained to partially drained or undrained penetration because of the insufficient maximum penetration rate. Kokusho et al. (2012) examined the influence of non/low-plastic fines on the cone resistance using a miniature cone in triaxial equipment. In this study, the cone diameter and penetration rate were small, which transmitted the drainage condition of silty soils from undrained to partially drained or drained despite the penetration being conducted into the highest fines content of 30%. Therefore, T values according to FC were not determined. Karaman (2013) and Ecemis and Karaman (2014) studied with the same field test results about the effects of FC and c_h on cone penetration and liquefaction resistance. They proposed the transition value 10 from partially drained to undrained penetration because there is no alteration in q_{c1N} above 10 of T . Especially for stiff dense to medium dense soils, q_{c1N} decreased with an increase in T between 10^{-3} and 10. Huang (2015) investigated the fines content (FC) effect on q_{c1N} of silty sands. It was determined that q_{c1N} decreases for a given D_r during partially drained penetration as T increases indicating that FC increases. From drained to undrained penetration, demarcation values for T are 0.04 and 10, respectively, according to Huang (2015).

In addition, Randolph and Hope (2004); Schneider et al. (2007), Thevanayagam and Ecemis (2008); Kim et al. (2008); Jaeger et al. (2010); Oliveira et al. (2011); Yi et al. (2012), and Cecceto and Simonini (2017) proposed similar transition values for T between drained and undrained penetration as seen in Table 4.1.

Table 4.1. T values from investigations in literature for undrained and drained penetration

Reference	Soil Type	Test Type	T for undrained	T for drained
Randolph and Hope, 2004	NC Clay	Centrifuge	>30	<0.3
Schneider et al., 2007	NC and OC Clay	Centrifuge	>100	-
Ecemis, 2008	Silty sand	Numerical	>5	<0.01
Kim et al., 2008	Clay	Calibration Chamber	>10	<0.05
Jaeger et al., 2010	Clay	Centrifuge	>20	<0.01
Oliveira et al., 2011	Clay	Centrifuge	>75	<1
Yi et al., 2012	-	Numerical	>10	<0.1
Cecceto and Simonini, 2017	-	Numerical	>60	<0.2
Taneri, 2021	Silty sand	Field Tests	>10	<0.001

As a result of comparison with whole investigations, the limit values of T obtained in this study verified the results for some ranges of average densities from Karaman (2013) and Ecemis and Karaman (2014), although different interpretations methods were used to determine the effect of c_h on q_{c1N} .

Even if loose silty sands had been tended to exist at bigger T values according to Karaman (2013) and Ecemis and Karaman (2014) in Figure 2.1, which was mentioned in Chapter 2, medium dense silty sands could be observed from drained to undrained penetration in this study. It was mentioned in Karaman (2013) and Ecemis and Karaman (2014) only D_r was a key parameter affecting the q_{c1N} of loose silty sands. However, it could be said that for medium dense to loose silty sands, both D_r and T influenced q_{c1N} and $\Delta u/\sigma_{v0}'$, which was occurred by the CPT probe. Thus, this inference provided to evaluate q_{c1N} and $\Delta u/\sigma_{v0}'$ obtained from the cone penetration under all conditions except much denser than 65% of silty sands.

In this study, it was concluded that from drained to undrained dissipation, q_{c1N} decreased, and $\Delta u/\sigma_{v0}'$ increased between 10^{-3} and 10 for all D_r values. This range showed the partially drained behavior of silty sands. This study indicated that the limit values of T could be applied to understand the change in q_{c1N} and $\Delta u/\sigma_{v0}'$ regardless of the relative density. At the same time, the change in q_{c1N} and $\Delta u/\sigma_{v0}'$ could be followed according to the relative density at the same T value.

4.3. Effect of Relative Density On q_{c1N} and $\Delta u/\sigma_{v0}'$

In this study, D_r was used to relate cone penetration resistance with densification of silty soil derived from Standard Penetration Test (SPT), as mentioned in Chapter 3. The variation of q_{c1N} with T for different average densities were plotted in Figure 4.5a, and $\Delta u/\sigma_{v0}'$ with T variation could be seen in Figure 4.5b in order to evaluate the effect of D_r on cone resistance.

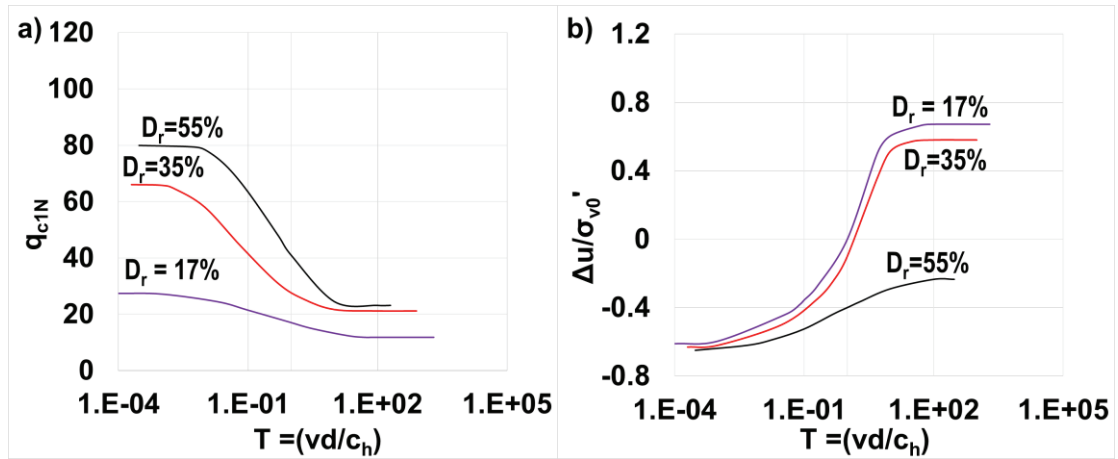


Figure 4.5. a) q_{c1N} and b) $\Delta u/\sigma_{v0}'$ with T for different average D_r values of 17%, 35% and 55%

$\Delta u/\sigma_{v0}'$ values for loose silty sands were observed from negative to positive when T was kept increasing in Figure 4.5b. However, $\Delta u/\sigma_{v0}'$ values for medium-dense soils were negative for both drained and undrained penetration. If $\Delta u/\sigma_{v0}'$ values had been obtained for more dense silty sands from Figure 4.5b, it could be mentioned based on the investigations of Huang (2015) and Thevanayagam and Ecmis (2008), respectively, in section 2.3 Figure 2.9 and section 2.2 Figure 2.8 that $\Delta u/\sigma_{v0}'$ was decreasing to negative values in the range of partially drained penetration. This result was explained as the dilative behavior of silty sands and the undrained response around the cone.

In contrast, $\Delta u/\sigma_{v0}'$ was negative below 10^{-3} of T as drained penetration in this study, but in Huang (2015) and Thevanayagam and Ecmis (2008), $\Delta u/\sigma_{v0}'$ was zero at the drained penetration range. Also, Krage and Dejong (2016) found similar results with Huang (2015) and Thevanayagam and Ecmis (2008). In addition, Krage and Dejong (2016) also said that the excess pore pressure tended to increase at a higher normalized penetration rate. However, Huang (2015) and Thevanayagam and Ecmis (2008)

proposed that even if the dilative behavior of silty sands caused to obtain the negative excess pore pressure, the negative excess pore pressure did not increase at undrained penetration, remained constant.

$\Delta u/\sigma_{v0}'$ did not vary too much when the relative density decreases, at the same T where is smaller than 10^{-3} in Figure 4.5b. However, when T was bigger than 10, $\Delta u/\sigma_{v0}'$ of 35% average density of silty sands was 4 times bigger than $\Delta u/\sigma_{v0}'$ of 55% average density of silty sands because of dilatation effect. Unlike, q_{c1N} had not been affected as the same proportion by the change in D_r . When T was bigger than 10, q_{c1N} of 35% average density of silty sands was 2 times bigger than q_{c1N} of 17% average density of silty sands as it can be seen in Figure 4.5a.

These proportions were more consistent between $\Delta u/\sigma_{v0}'$ and q_{c1N} compared to other investigations. Thevanayagam and Ecmis (2008) and Huang (2015) showed similar inferences with these results according to $\Delta u/\sigma_{v0}'$. However, the change in q_{c1N} between nearly 10% and 35% of relative densities did not compare to the results of this study. For example, the result of this study contradicted that the result of Karaman (2013) and Ecmis and Karaman (2014) for below D_r of 40%. For normally consolidated and contractive soils, Krage and Dejong (2016) suggested a ratio of q_{c1N} for drained to undrained penetration was in the range 1.3 to 3 regardless of the relative density. However, in this study, q_{c1N} values belonged to 35 % and 55% D_r decreased much more than the ratio of Krage and Dejong (2016).

According to inferences obtained from Chapter 3, it was thought that D_r of fine-grained sands was the issue about the occurrence of different types of dissipation curves. In addition, it could be seen that PPDT was helpful to determine T values from partially to undrained penetration for loose sands to medium dense sands in Figure 4.1a and Figure 4.1b. Otherwise, for loose to medium dense silty sands, DPPT was profit to evaluate q_{c1N} from drained to partially drained penetration as it can be clearly seen in Figure 4.1c. The result could be taken that PPDT was considerably affected by D_r of silty sands. Therefore, for partially drained and drained silty sands, DPPT was helpful to understand T values for all relative densities. For undrained drainage conditions, PPDT could be applied to specify the relative density of silty sands. And also, $\Delta u/\sigma_{v0}'$ graphs encouraged this result by showing the same behavior of q_{c1N} .

4.4. Conclusion

This chapter examined the effects of c_h and D_r on q_{c1N} and $\Delta u/\sigma_{v0}'$ of silty sands and clean sands. According to comparisons, it was seen that;

- T demarcation values obtained from this study were 10^{-3} and 10 for drained to undrained penetration, respectively. As the T value increased, q_{c1N} decreased, and $\Delta u/\sigma_{v0}'$ increased between this range with respect to their D_r values.
- The method of Chai et al. (2012) was more consistent to evaluate the dissipation pore pressure gives the non-standard curve than the method belongs to Sully et al. (1999)
- Both T and D_r were influencers about the cone resistance and excess pore pressure for medium to loose silty sands except denser than 65% D_r values.
- Dilative behavior was the effect on excess pore pressure with respect to drainage conditions of silty sands. However, more dense silty sands were needed to investigate the effect of excess pore pressure induced around the cone on the cone resistance during penetration.
- The change in $\Delta u/\sigma_{v0}'$ was consistent according to their relative densities with literature, but for undrained penetration, q_{c1N} was not affected from as the same proportion as excess pore pressure with increasing in D_r values.
- PPDT was applicable for undrained to partially drained, and DPPT was applicable for partially drained to drained penetration. Partially drained behavior of silty sands at the standard penetration rate of 2 cm/sec could be observed based on both PPDT and DPPT.

CHAPTER 5

CONCLUSION AND RECOMMENDATION FOR FUTURE STUDY

5.1. Summary of The Study

In this investigation, field tests were conducted for silty sands and clean sands to determine the effects of coefficient of consolidation and the relative density on the cone resistance and excess pore pressure induced around the cone during the penetration.

First of all, the relation was established between the cone resistance or excess pore pressure and consolidation characteristics of silty sands using non-dimensional penetration rate. Because of using the same results to estimate the effect of coefficient of consolidation on the cone resistance, the comparisons were done between Karaman (2013) and this study as follows;

- The first result obtained from graphs was that the demarcation non-dimensional penetration rate of silty sands from partially drained to undrained penetration was same as 10 with Karaman (2013). However, Karaman (2013) did not propose any transition value from drained to partially drained condition because different drained behavior was observed under different ranges of average relative densities. In this study as different, the limit penetration rate value was proposed as 10^{-3} from drained to partially drained by using the study of Arık (2021).
- The second result of this relation was that Chai et al. (2012) was more applicable than the method of Sully et al. (1999) in order to estimate coefficient of consolidation of non-standard dissipation curves obtained from pore pressure dissipation tests for silty sands.
- As the last one was that the cone resistance decreased and excess pore pressure increased between these values as the non-dimensional penetration rate increased with respect to related the relative density. At the same time, it was seen that both the non-dimensional penetration rate and the relative density affected the cone

resistance and excess pore pressure from medium dense to loose silty sands except denser than the relative density of 65% value.

Secondly, it had been obviously seen that the relative density has an effect on the cone resistance and excess pore pressure depending on the relation mentioned above.

- When the relative density increased, the change in excess pore pressure decreased and undrained excess pore pressure values were calculated as negative. Dilative behavior in silty sands caused this behavior of excess pore pressure.
- The cone resistance and excess pore pressure were differently affected by the change in the relative density with respect to drainage conditions. The change in excess pore pressure was consistent when it is compared to literature. However, the cone resistance did not show the similar proportion.
- The non-dimensional penetration rate of partially drained could be calculated using both pore pressure dissipation test and direct push permeability test at standard penetration rate of 2 cm/sec. Nevertheless, pore pressure dissipation test was appropriate for undrained and direct push permeability test was appropriate for drained penetration.

5.2. Recommendation for Future Study

- More dense silty sands are needed to investigate the effect of dilation on excess pore pressure induced around the cone and therefore to explain the effect of excess pore pressure on the cone resistance during penetration.
- In literature, the non-standard dissipation curve is caused by density of sandy soils or consolidation characteristic of clayey soils. However, in this study, undrained penetration in medium dense soils was not obtained even if a few of non-standard curves were observed during the analysis of dissipation test results. The reason of non-standard curves has to be investigated in silty soils.
- The cone resistance and excess pore pressure under drained penetration can be investigated using same interpretation methods in order to estimate the limit non-dimensional penetration rate combining graphs plotted in this study.

REFERENCES

- Arık, M.S. (2021) *Effect of fines content on CPT resistance in silty sands*. Master Thesis, Izmir Institute of Technology, Izmir.
- ASTM D-2487 *Standard practice for classification of soils for engineering purposes (unified soil classification system)*. ASTM International, West Conshohocken, PA, 2017.
- ASTM D-5778 *Standard test method for electronic friction cone and piezocone penetration testing of soils*. ASTM International, West Conshohocken, PA, 2020.
- ASTM D-6067 *Standard practice for using the electronic piezocone penetrometer tests for environmental site characterization and estimation of hydraulic conductivity*. ASTM International, West Conshohocken, PA, 2017.
- ASTM D-1586 *Standard test method for standard penetration test (SPT) and split-barrel sampling of soils*. ASTM International, West Conshohocken, PA, 2018.
- Baligh, M.M., Azzouz, A.S., Wissa, A.Z.E., Martin, R.T., Morrison, M.J. (1981) *The piezocone penetrometer*. Massachusetts Institute of Technology.
- Boulanger, R.W. (2003) *High overburden stress effects in liquefaction analyses*. Journal of Geotechnical and Geoenvironmental Engineering, ASCE, Vol.129(12), 1071-1082.
- Bugno, W.T. and McNeilan, T.W. (1984) *Cone penetration test results in offshore California silts, Strength testing of Marine Sediments; Laboratory and In situ Measurements*. Symposium San Diego 1984, ASTM Special technical publication, STP 883, 55-71.

- Burns, S.E., Mayne, P.W. (1998) *Monotonic and dilatatory pore pressure decay during piezocone tests in clay*. Canadian Geotechnical Journal, 35(6), 1063-1073.
- Cecceto, F., Simonini, P. (2017) *Numerical study of partially drained penetration and pore pressure dissipation in piezocone test*. Acta Geotechnica, 12(1), 195-209.
- Chai, J., Sheng, D., Carter, J.P., Zhu, H. (2012a) *Coefficient of consolidation from non-standard piezocone dissipation curves*. Computers and Geotechnics. Vol. 41, 13-22.
- Cubrinovski, M. and Ishihara, K. (1999) *Empirical correlation between SPT N-value and relative density for sandy soils*. Japanese Geotechnical Society, Soils and Foundations, Vol.39 No.5, 61-71
- Das, B.M. (2007) *Principles of Foundation Engineering, 6th Edition*.
- Dejong, J.T., and Randolph, M. (2012) *Influence of partial consolidation during cone penetration on estimated soil behavior type and pore pressure dissipation measurements*. Journal of Geotechnical and Geoenvironmental Engineering, ASCE, Vol.138(7), 777-788.
- Ecemis, N. (2013) *Effects of consolidation characteristics on CPT cone resistance and liquefaction resistance in silty soil*. The Scientific and Technological Research Council of Turkey-TUBITAK, Project No: 110M602, Ankara, Türkiye.
- Ecemis, N. (2014) *Effects of permeability and compressibility on liquefaction assessment of silty soils using cone penetration resistance*. European Union FP7-PEOPLE-2009-Reintegration Grant Project Report, Project No: 248218, Brussels, Belgium.
- Ecemis, N. and Karaman, M. (2014) *Influence of non-/low plastic fines on cone penetration and liquefaction resistance*. Engineering Geology, 48-57.

- Finnie, I.M.S. and Randolph, M.F. (1994) *Punch-through and liquefaction induced failure of shallow foundations on calcareous sediments*. Proc. Int. Conf. On Behaviour of Offshore Structures, Boston, 217-230.
- Ha, T-G., Jang, I-S., Choo, Y-S., Chung, C-K. (2014) *Evaluation of coefficient of consolidation for dilatatory dissipation in piezocone test in over consolidated cohesive soils*. KSCE Journal of Civil Engineering, Vol.18(2), 475-487.
- House, A.R., Oliveira, J.R.M.S., Randolph, M.F. (2001) *Evaluating the coefficient of consolidation using penetration tests*. Int. J. of Physical Modelling in Geotechnics, Vol. 1, No.3, 17-25.
- Huang,Q. (2015) *Effect of non-plastic fines on cone resistance in silty sands*. Ph.D. dissertation. State University of New York.
- Jaeger, R.A., Dejong, J.T., Boulanger, R.W., Low, H.E., Randolph, M.F. (2010) *Variable penetration rate CPT in an intermediate soil*. Proc. 2nd Int. Symp. on Cone Penetration Testing.
- Karaman, M. (2013) *Effects of consolidation characteristics on CPT cone resistance and liquefaction resistance in silty soils*. Master Thesis, Izmir Institute of Technology, Izmir.
- Kibria, S. and Masood, T. (1998) *SPT, relative density and PHI relationships for indus sands at Chashma*. Proceeding of VII National Conference of Pakistan National Society for Soil Mechanics and Foundation Engineering, 169-188.
- Kim K., Prezzi, M., Salgado, R., Lee, W. (2008) *Effect of penetration rate on cone penetration resistance in saturated clayey soils*. Journal of Geotechnical and Geoenvironmental Engineering, ASCE, 134(8),1142-1153.
- Kokusho, T., Ito, F., Nagao, Y., Green, A.R. (2012) *Influence of non/low plastic fines and associated aging effects on liquefaction resistance*. Journal of Geotechnical and Geoenvironmental Engineering, 138(6), 747-755.

- Krage, C.P., Dejong, J.T. (2016) *Influence of drainage conditions during cone penetration on the estimation of engineering properties and liquefaction potential of silty and silty soils*. Journal of Geotechnical and Geoenvironmental Engineering, ASCE, 142(11), 04016059.
- Kulhawy, F.H. and Mayne, P.W. (1990) Manual on Estimating Soil Properties for Foundation Design, Final Report (EL-6800) submitted to Electric Power Research Institute (EPRI), Palo Alto, Calif.
- Kumar, J. and Bajju, K.V.S.B. (2009) *Penetration rate effect on miniature cone tip resistance for different cohesionless material* Geotechnical Testing Journal, 32(4),1-10.
- Lee, D.S., Elsworth, D., Hryciw, R. (2008) *Hydraulic conductivity measurement from on the-fly uCPT sounding and from VisCPT*. Journal of Geotechnical and Geoenvironmental Engineering, ASCE, 1720-1729.
- Lunne, T., Robertson, P.K., Powell, J.J.M. (1997). *Cone penetration testing in geotechnical practice*.
- Mahmoodzadeh, H., Randolph, M.F., Wang, D. (2014) Numerical simulation of piezocone dissipation test in clays. Geotechnique, Vol.64(8), 657-666.
- Meyerhof, G.G. (1956) *Penetration tests and bearing capacity of cohesionless soils*. Journal of Geotechnical Engineering, ASCE, Vol.82 No.1, 1-19.
- Mujtaba, H., Farooq, K., Sivakugan, N., Das, B.M. (2018) *Evaluation of relative density and friction angle based on SPT-N values*. KSCE Journal of Civil Engineering, Vol.22(2), 572-581.
- Oliveira, J.R.M.S., Almeida, M.S.S., Motta, H.P.G., Almeida, M.C.F. (2011) *Influence of penetration rate on penetrometer resistance*. Journal of Geotechnical and Geoenvironmental Engineering, ASCE, 137(7), 695-703.

- Oliveira, J.R.M.S., Almeida, M.S.S. Marques, M.E.S., Almeida, M.C.F. (2006) *Undrained strength of very soft clay soils used in pipeline studies in the centrifuge*. 6th International Conference on Physical Modelling in Geotechnics, Taylor&Francis, London, 1355-1369.
- Parez, L., Fauriel, L. (1988) *Le piezocone ameliorations apportees a la reconnaissance de sols*. Revue Francaise de Geotech., Vol. 44, 13-27.
- Randolph, M.F. and Hope, S. (2004) *Effect of cone velocity on cone resistance and excess pore pressures*. Proc. Int. Sym. On Eng. Practice and Performance of Soft Deposits, Osaka, 147-152.
- Robertson, P.K. (2009) *Interpretation of cone penetration tests-a unified approach*. Canadian Geotechnical Journal, Vol.46(11), 1337-1355.
- Robertson, P.K. and Wride, C.E. (1998) Evaluating cyclic liquefaction potential using the cone penetration test. Canadian Geotechnical Journal, Vol.35(3), 442-459.
- Schneider, J.A., Lehane, B.M., Schnaid, F. (2007) *Velocity effects on piezocone measurements in normally and over consolidated clays*. Int. J. Physical Model. in Geotechnics., 7(2),23-34.
- Skempton, A.W. (1986) *Standard penetration test procedures and the effect in sands of overburden pressure, relative density, particle size, aging and overconsolidation*. Geotechnique, Vol.36 No.3, 425-447.
- Sully, J.P., Robertson, P.K., Campanella, R.G., Woeller, D.J. (1999) *An approach to evaluation of field CPTU dissipation data in overconsolidated fine-grained soils*. Canadian Geotechnical Journal, 37(6), 369-381.
- Teh, C.I., and Houlsby, G.T. (1991) *An analytical study of cone penetration test in clay*. Geotechnique, 41(1), 17-34.

- Thevanayagam, S., Ecmis, N. (2008) *Effects of permeability on liquefaction resistance and cone resistance*. Geotechnical Earthquake Engineering and Soil Dynamics IV, 1-11.
- Wroth, C.P. (1984) *The interpretation of in situ soil test*. Geotechnique, Vol.34(4), 449-489.
- Yi, J.T., Goh, S.H., Lee, F.H., Randolph, M.F. (2012) *A numerical study of cone penetration in fine-grained soils allowing for consolidation effects*. Geotechnique, 62(8), 707-719.
- Youd, T.L., Idriss, I.M. (2001) *Liquefaction resistance of soils: Summary report from the 1996 NCEER and 1998 NCEER/NSF workshops on evaluation of liquefaction resistance of soils*. Journal of Geotechnical and Geoenvironmental Engineering, ASCE, Vol.127, 297-3.

APPENDICES

APPENDIX A

CORRECTED STANDARD PENETRATION NUMBERS AND RELATIVE DENSITIES

Table A.1. N_{60} and D_r values obtained from field tests on the Northern side of Izmir Gulf performed in 2013 by Ecemis et al.

Borehole Number	Depth(m)	(N)60	Dr(%)	Borehole Number	Depth(m)	(N)60	Dr(%)
SC1	3	7.82	21.36	SC7	5.25	2.40	12.25
SC1	3.5	7.82	21.82	SC7	5.75	21.33	49.73
SC1	4	7.82	22.24	SC7	6.25	21.33	50.08
SC1	5	12.10	31.40	SC7	6.75	21.33	50.39
SC2	3	5.53	17.65	SC7	11.75	12.07	34.46
SC2	3.5	5.53	18.03	SC8	3	4.56	14.49
SC2	4	5.53	18.39	SC8	5	7.87	22.73
SC3	4.25	11.53	30.76	SC8	7	8.50	25.26
SC3	4.7	11.53	31.03	SC8	9.5	8.00	25.51
SC3	5.2	11.53	31.31	SC8	10	8.00	25.69
SC3	6.15	5.56	20.08	SC8	11.5	7.10	24.45
SC3	6.7	5.56	20.32	SC8	12	8.07	26.51
SC3	7.2	5.56	20.52	SC9	5.5	5.69	18.81
SC3	7.7	7.30	24.11	SC9	7	1.18	10.88
SC3	8.2	7.30	24.29	SC9	7.75	1.65	12.18
SC3	8.7	9.20	28.21	SC9	8.5	1.65	12.50
SC3	9.2	9.20	28.37	SC9	9.25	3.62	16.67
SC3	9.86	9.20	28.58	SC9	10.5	3.41	16.74
SC4	2.5	4.39	14.42	SC9	11.5	3.41	17.09
SC4	3.5	4.39	15.34	SC10	2.75	2.59	10.46
SC4	6	10.38	28.79	SC10	3.25	2.59	10.99
SC4	7	10.38	29.37	SC10	4.25	2.59	11.89
SC4	10	12.11	34.10	SC10	5.75	2.25	12.29
SC4	10.5	10.08	30.28	SC10	6.25	2.25	12.59
SC4	11.5	10.08	30.57	SC11	2.5	9.61	23.89
SC4	12.25	3.91	18.67	SC11	4.5	4.72	16.28
SC5	2	11.18	26.27	SC11	5.5	4.72	16.98
SC5	2.5	11.18	26.92	SC11	6.5	11.03	29.98
SC5	3.25	3.87	13.43	SC11	7.5	3.08	14.89
SC5	4	3.87	14.14	SC11	8.5	3.08	15.32
SC5	4.75	2.40	11.86	SC11	9.5	12.12	33.43
SC5	6	2.40	12.70	SC11	12.5	21.91	53.80
SC5	7	6.31	20.89	SC11	13.5	20.84	52.00
SC5	9.5	1.98	13.55	SC11	14.5	20.84	52.26
SC5	10.75	4.68	19.29	SC11	15.5	19.91	50.68
SC5	11.5	4.68	19.53	SC11	16.5	19.91	50.93
SC6	1.75	7.68	19.14	SC12	1	7.32	14.97
SC6	10.25	5.83	21.94	SC12	2	7.32	17.46
SC6	10.75	7.37	25.11	SC12	4	19.54	44.19
SC7	2.5	4.89	10.09	SC12	5	14.99	36.22
SC7	3.25	2.58	10.92	SC12	6	4.08	15.67
SC7	3.75	2.58	11.40	SC12	7	4.08	16.31
SC7	4.5	2.40	11.68	SC12	8	22.44	52.88

(cont. on next page)

Table A.1 (cont.)

Borehole Number	Depth(m)	(N)60	Dr(%)	Borehole Number	Depth(m)	(N)60	Dr(%)
SC12	9	15.47	39.66	SC17	9.25	12.60	34.55
SC12	12	16.08	42.01	SC17	10.75	14.09	38.03
SC12	14	14.92	40.40	SC17	12.25	5.57	21.76
SC12	15	14.92	40.68	SC17	13.75	9.30	29.51
SC13	6.75	3.28	14.67	SC17	15	4.60	20.57
SC13	7.75	3.06	14.73	SC17	16.25	4.60	20.82
SC13	8.75	1.92	12.95	SC18	3.25	2.00	9.10
SC13	10.75	10.92	31.34	SC18	4.75	2.48	11.53
SC13	16.75	7.89	27.17	SC18	6.25	4.05	15.70
SC14	2.25	17.48	39.89	SC18	7.75	8.66	25.70
SC14	3.25	17.48	41.06	SC18	8.5	8.66	26.06
SC14	4	17.48	41.66	SC18	10	4.58	18.73
SC14	4.75	11.05	29.59	SC18	10.75	12.01	33.57
SC14	5.25	11.05	29.90	SC18	11.25	12.01	33.74
SC14	7.75	15.87	40.60	SC18	12.25	2.28	14.97
SC14	8.5	15.87	40.93	SC18	13.75	12.57	35.58
SC14	9.25	16.42	42.31	SC18	15	6.20	23.39
SC14	10	16.42	42.56	SC18	16.25	6.20	23.67
SC14	13	19.40	49.32	SC19	2	2.79	10.02
SC14	13.75	19.40	49.53	SC19	3.25	5.80	17.43
SC15	3.25	6.59	18.92	SC19	4.75	12.07	31.09
SC15	4	6.59	19.59	SC19	5.5	12.07	31.61
SC15	4.75	7.97	22.92	SC19	6.25	11.34	30.67
SC15	5.5	7.97	23.40	SC19	7	11.34	31.08
SC15	6.25	3.44	14.95	SC19	7.75	12.30	33.31
SC15	7.75	14.00	36.48	SC19	8.5	12.30	33.63
SC15	12.25	17.31	44.76	SC19	9.25	14.60	38.42
SC15	14	6.07	23.24	SC19	10.75	4.75	19.64
SC15	15	9.09	29.40	SC19	12.25	6.70	23.90
SC15	16	9.09	29.62	SC19	13.75	5.47	21.91
SC16	5.5	6.80	22.11	SC19	15	3.58	18.51
SC16	6.25	11.71	32.14	SC19	16.25	3.58	18.77
SC16	7	11.71	32.50	SC20	1.75	3.53	10.65
SC16	7.75	13.53	36.38	SC20	2.75	5.87	16.63
SC16	8.5	13.53	36.65	SC20	3.75	5.87	17.69
SC16	9.25	21.41	52.39	SC20	5.75	6.24	20.08
SC16	10	21.41	52.65	SC20	6.75	6.24	20.63
SC16	10.75	17.12	44.49	SC20	7.75	10.64	29.74
SC16	11.5	17.12	44.68	SC20	8.75	12.11	33.04
SC16	12.25	2.97	17.14	SC20	9.75	12.11	33.47
SC16	13.75	4.86	21.19	SC20	10.75	4.77	19.46
SC16	16	27.89	66.87	SC20	12.75	6.78	24.11
SC17	7.75	12.30	33.33	SC20	13.75	5.64	22.15
				SC20	14.75	5.64	22.41

APPENDIX B

UNDRAINED-PARTIALLY DRAINED DISSIPATION CURVES

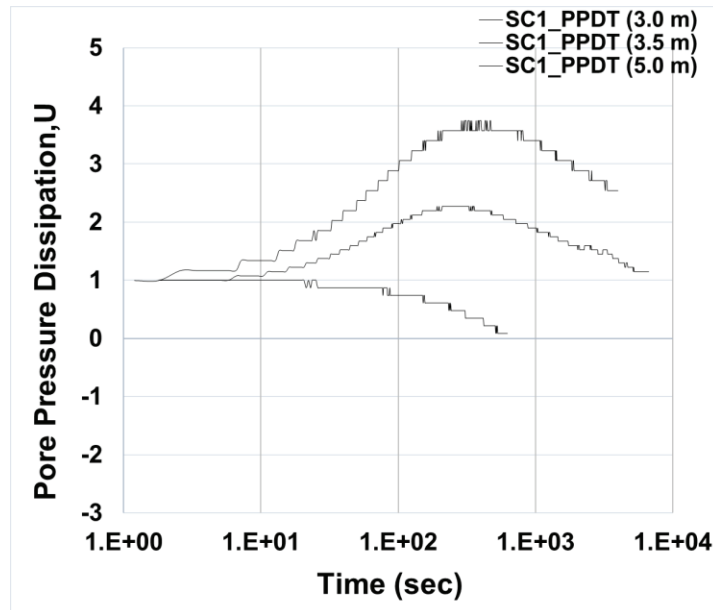


Figure B.1. Dissipation curves of SC1 borehole

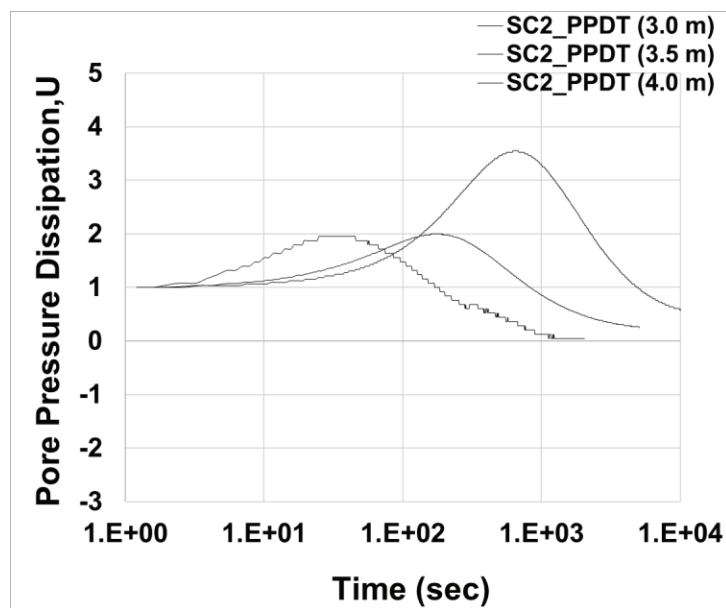


Figure B.2. Dissipation curves of SC2 borehole

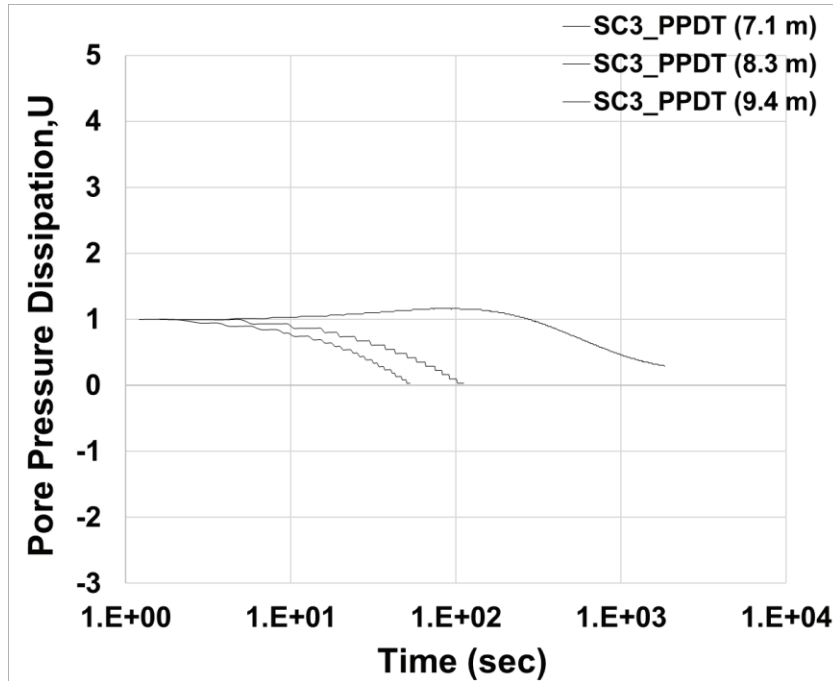


Figure B.3. Dissipation curves of SC3 borehole

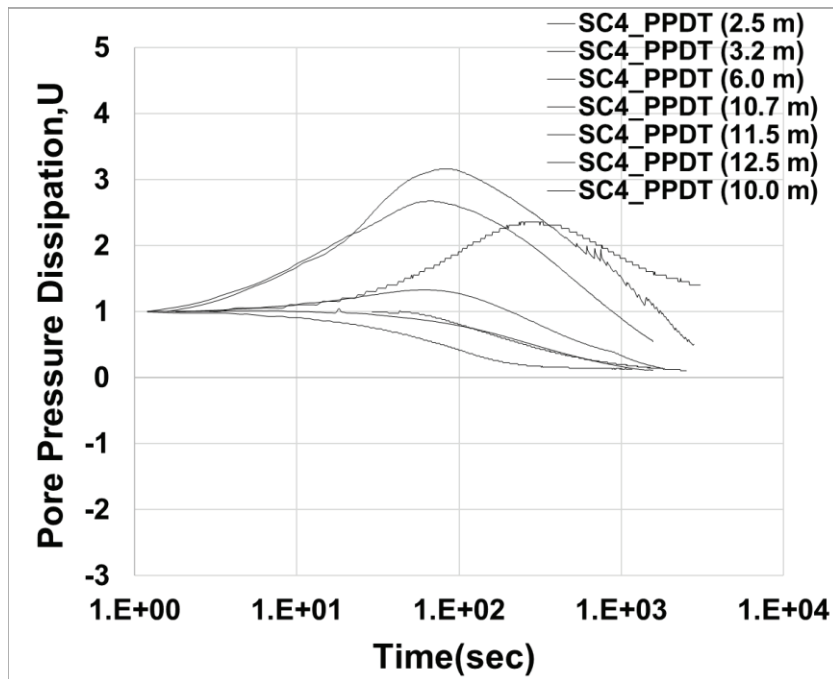


Figure B.4. Dissipation curves of SC4 borehole

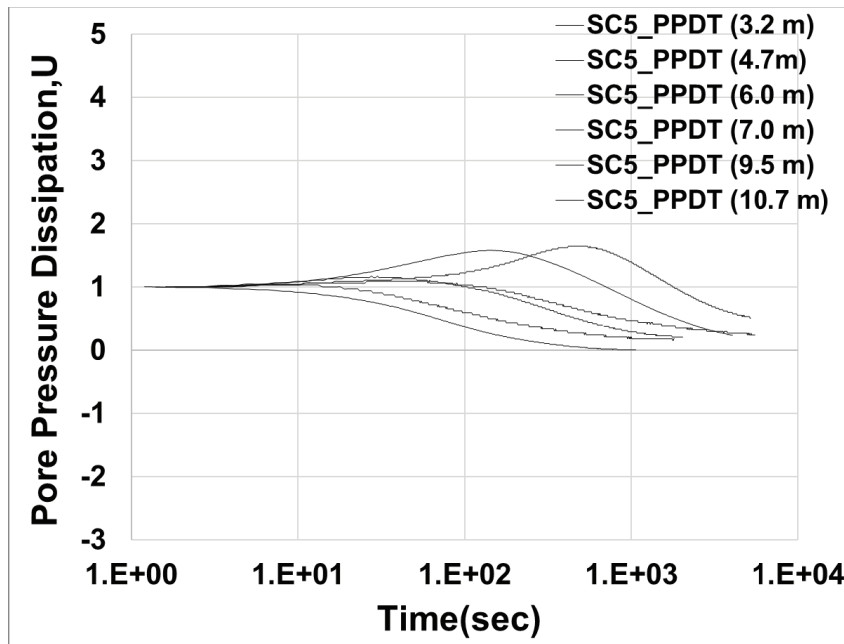


Figure B.5. Dissipation curves of SC5 borehole

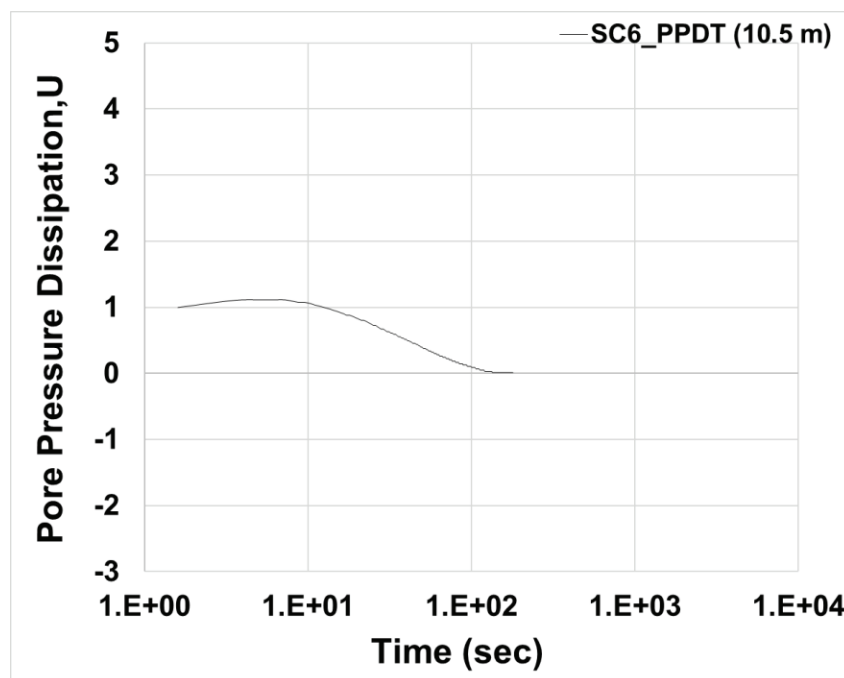


Figure B.6. Dissipation curves of SC6 borehole

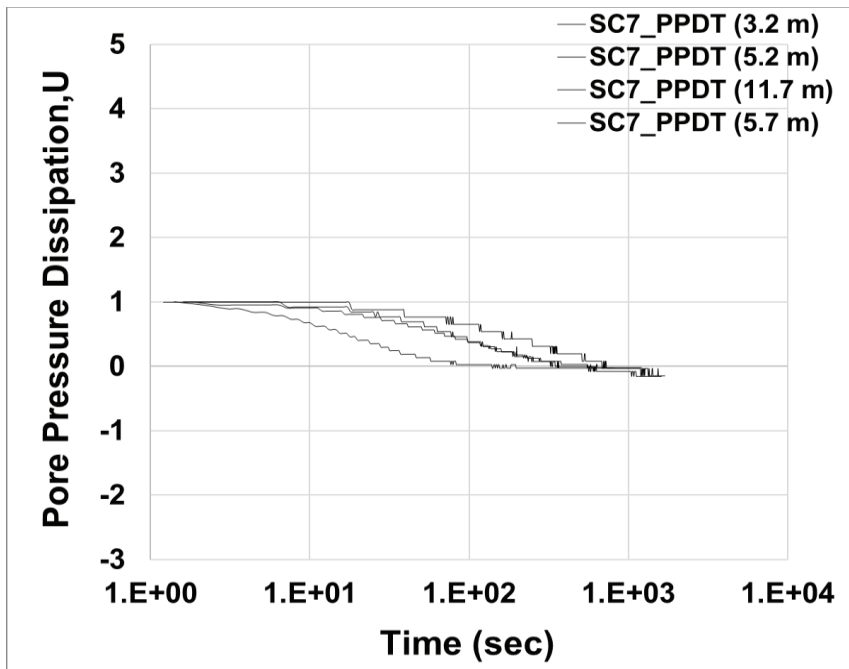


Figure B.7. Dissipation curves of SC7 borehole

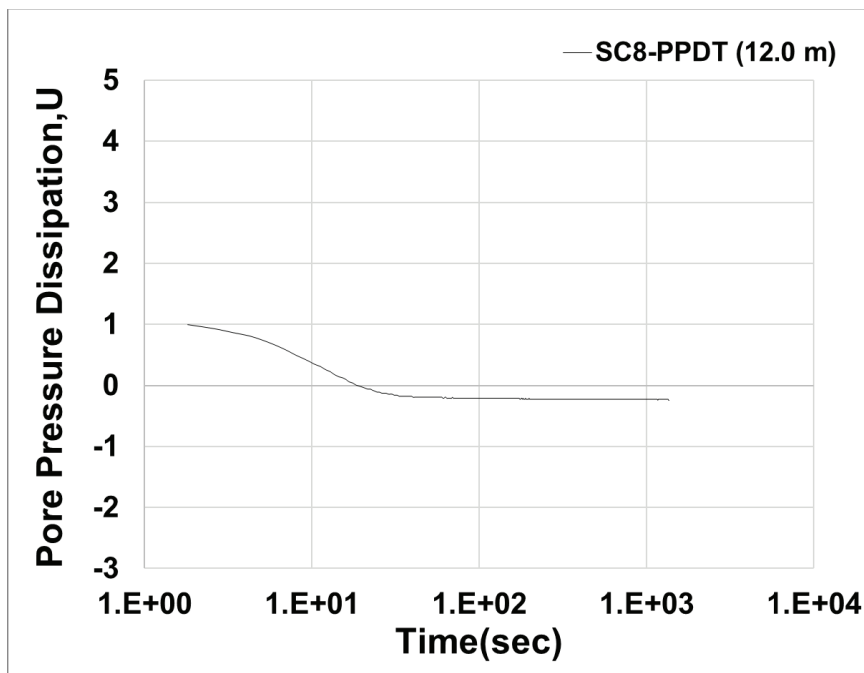


Figure B.8. Dissipation curves of SC8 borehole

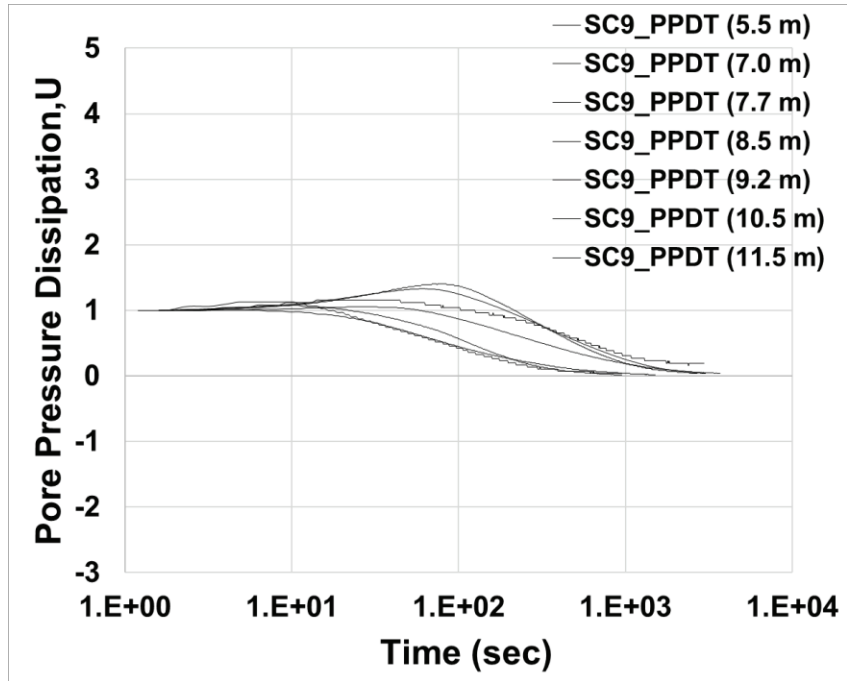


Figure B.9. Dissipation curves of SC9 borehole

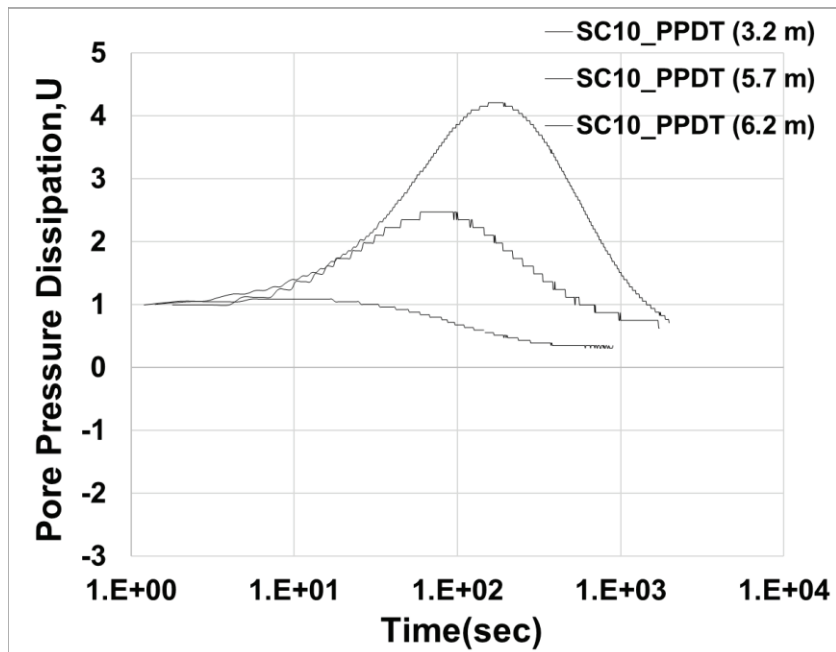


Figure B.10. Dissipation curves of SC10 borehole

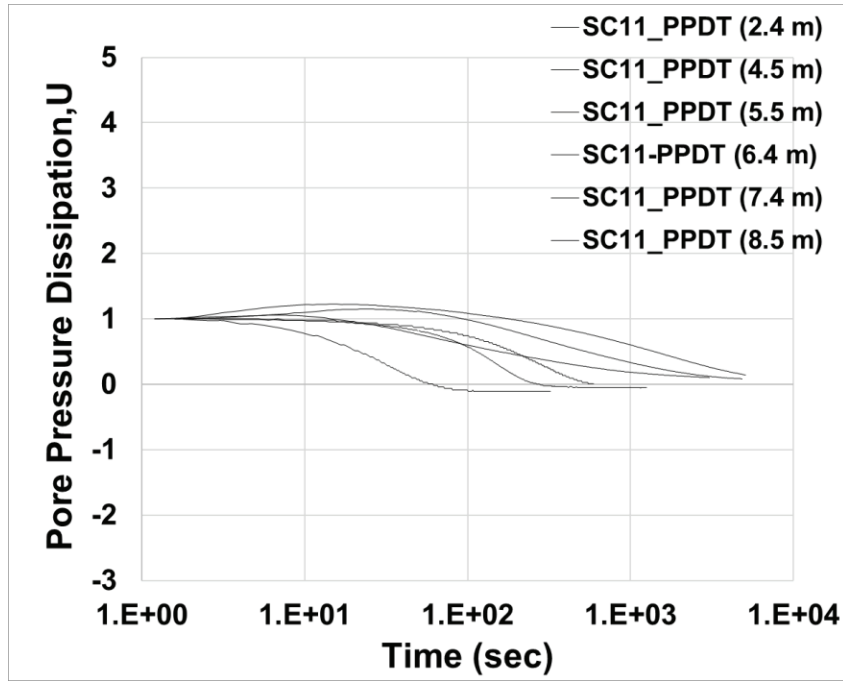


Figure B.11. Dissipation curves of SC11 borehole

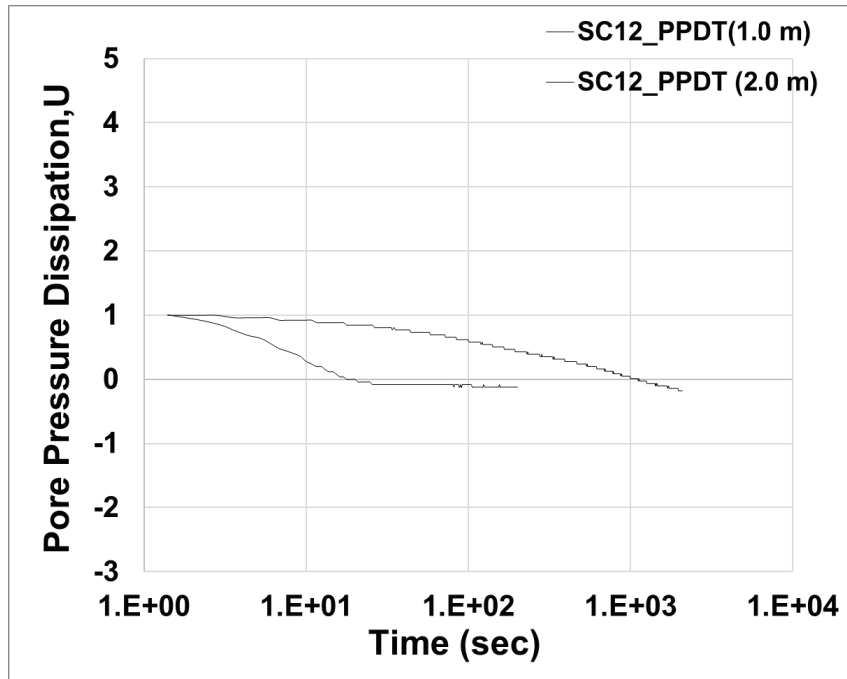


Figure B.12. Dissipation curves of SC12 borehole

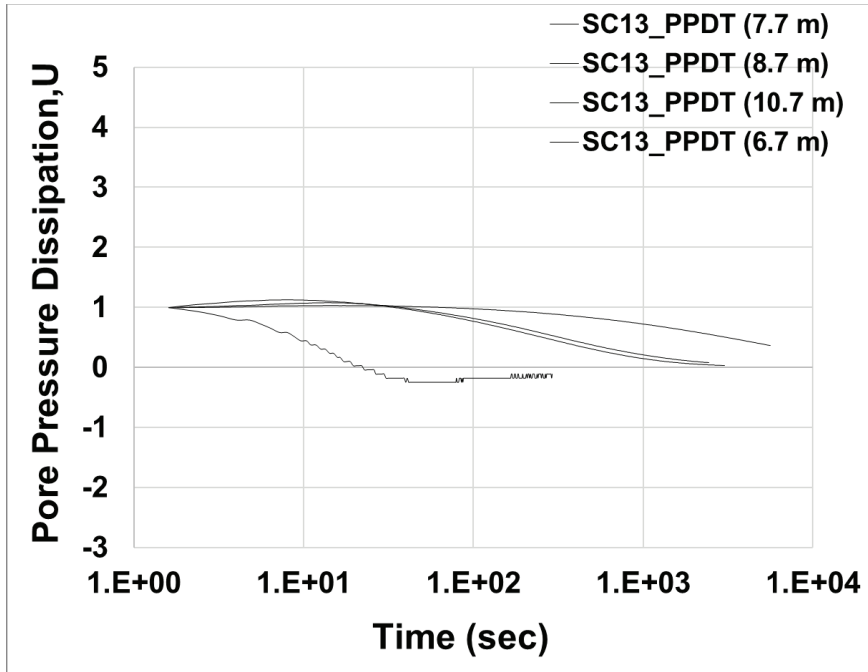


Figure B.13. Dissipation curves of SC13 borehole

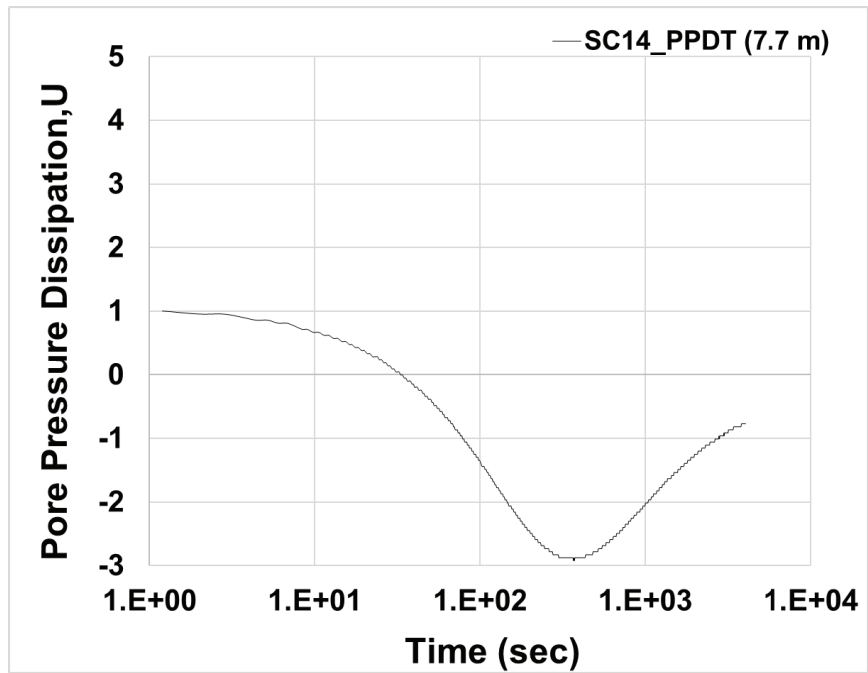


Figure B.14. Dissipation curves of SC14 borehole

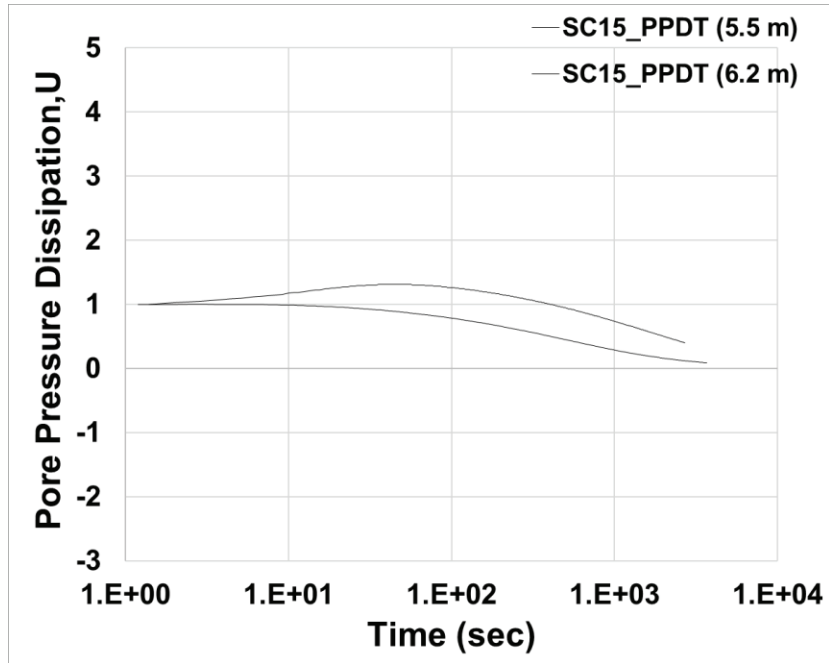


Figure B.15. Dissipation curves of SC15 borehole

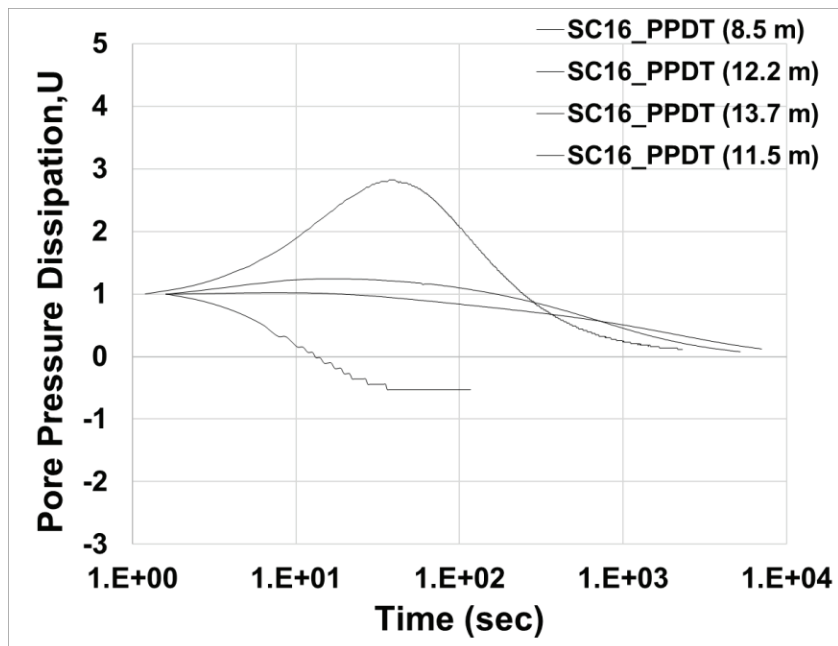


Figure B.16. Dissipation curves of SC16 borehole

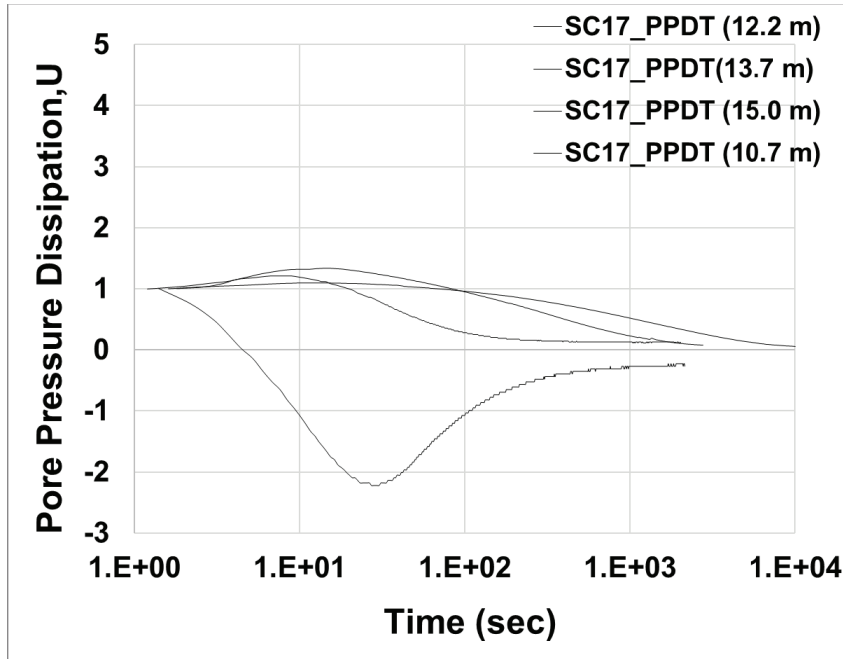


Figure B.17. Dissipation curves of SC17 borehole

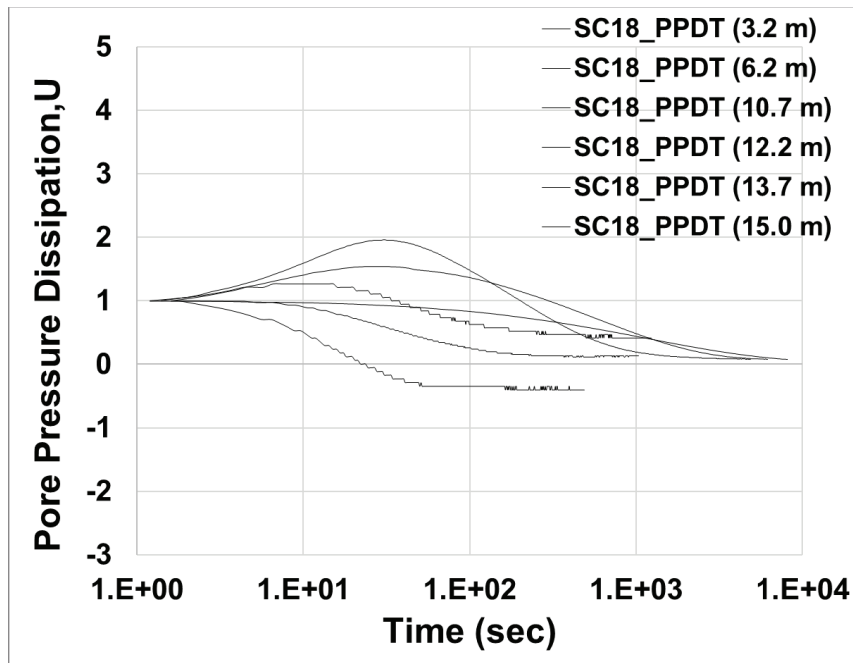


Figure B.18. Dissipation curves of SC18 borehole

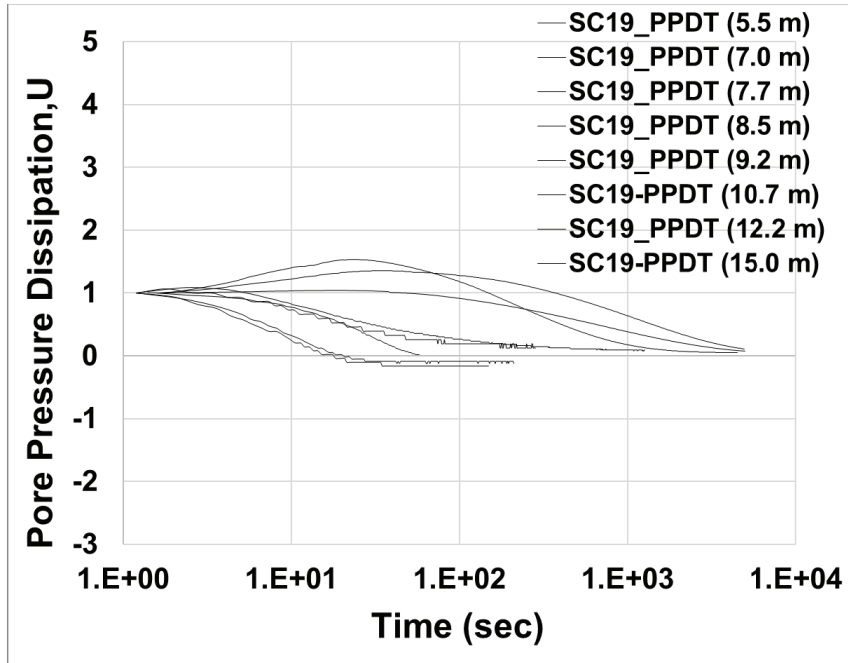


Figure B.19. Dissipation curves of SC19 borehole

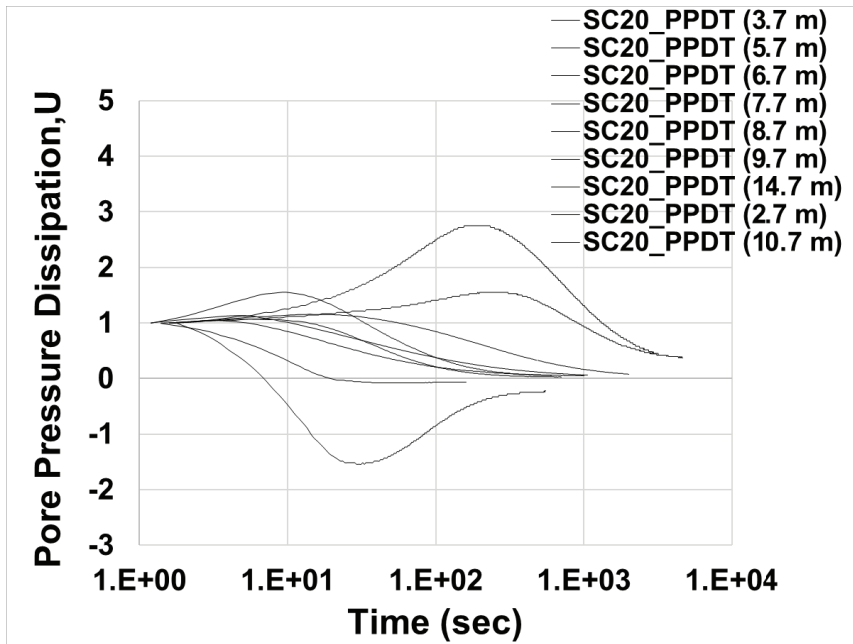


Figure B.20. Dissipation curves of SC20 borehole